P.J. de Bruijn

Compound weirs

Analytical and experimental research on stage-discharge relations

TU Delft

Compound weirs

Analytical and experimental research on stage-discharge relations

By

P.J. de Bruijn

4864034

in partial fulfilment of the requirements for the degree of

Bachelor of Science
in Civil Engineering

at the Delft University of Technology,

Supervisors: Prof.dr.ir. W.S.J. Uijttewaal
Dr.ir. D. Wüthrich

TU Delft

Preface

Before you lies the BSc thesis: “Compound weirs: Analytical and experimental research on stage-discharge relations”. This thesis is written to the end of completing the Civil Engineering bachelor at Delft University of Technology.

I would like to thank my first supervisor prof.dr.ir. Wim Uijttewaal for presenting me with this subject and for supporting me with my thesis through many meetings. Secondly, I would like to thank my second supervisor dr.ir. Davide Wüthrich for his help and feedback. I would also like to thank Chantal Willems and Pieter van der Gaag for their help with the experiment in the laboratory, which I would not have been able to carry out without them. Finally, I would like to thank my brother Kevin de Bruijn for his feedback on my thesis.

Almere, October 2021
Patrick de Bruijn

Summary

Two control structures in the form of compound weirs were built near Pannerden and in the Hondsbroeksche Pleij. These compound weirs consist of multiple adjacent gates with individually configurable weir heights. To make optimal use of the flexibility of the structures, research must be done into how different compound weir configurations affect the stage-discharge relationship. Both perfect and imperfect flow are researched.

This thesis has the following research question: *"How is the flow over a compound weir affected by the configuration of the individual weirs?"*

The research on imperfect weirs was caried out by constructing two analytical models based on a combination of momentum- and energy conservation, and a combination of Carnot losses and energy conservation. This was done for two cases, one case in which the equations were solved explicitly by using the average weir height, and the second case in which the equations were solved by solving a system of equations (one for each gate). The research on perfect weirs was caried out by making use of the Rehbock formulation, again for both the individual weir heights and the average weir height. To validate the models and to research interaction between adjacent gates, experiments were carried out in a 3-meter-wide flume with a scale model of the control structure near Pannerden.

In the experiments it was found that in the case of perfect weir flow, the discharge coefficients hardly change for different configurations with the same average weir height. The recorded maximum change was 1.9%. The best performing model for perfect flow was the model based on the average weir height. In the case of imperfect flow, it was found that the discharge coefficient can vary up to 13%, so the configuration influences the discharge coefficient significantly. No unambiguous results were found on how certain configurations affect the discharge coefficient. The models for imperfect flow performed well for an average weir height of 10 cm, but not for an average weir height of 7.5 cm. The least performing model was the model based on individual gates with the momentum equation.

With PIV (Particle Image Velocimetry) it was found that lateral flow starts at a greater distance from the weir if the lateral travelling distance is bigger. Furthermore, the streamlines hit the weir at an increased angle if the transition between high and low weir heights was sudden instead of gradual.

Further research should focus on adding more forms of energy head loss to the analytical model. Focus should be on one specific average weir height and more data should be collected on fewer configurations to get more insight into the behaviour caused by specific properties of a configuration.

Contents

1. Introduction

A compound weir is a combination of weirs that can take on arbitrary shapes. Such weirs are used to dynamically control the water level for different types of users or for varying circumstances, or for accurate flow measurements in open channels (Piratheepan et al., 2006). Shapes can be a triangle, to quadratically increase the cross-area of the weir with increasing water level.

Two other specific examples of a compound weir are found in the Hondsbroeksche Pleij (Figure 1) (Swart, 2019) and next to the Pannerdensch kanaal. These structures consist of multiple, parallel, sharp-crested weirs (Jansen, 2020) that can be modified to allow for dynamical control of the water level during periods of high-water. This is done to make sure the discharge is distributed as predetermined: 1/3 to the Pannerdensch kanaal and 2/3 to the river Waal (Rijkswaterstaat, 2021) in the case of the control structure near Pannerden. During periods of high-water, the floodplains are inundated and the ability to control the discharge distribution used to be reduced, which is why these control structures were built.

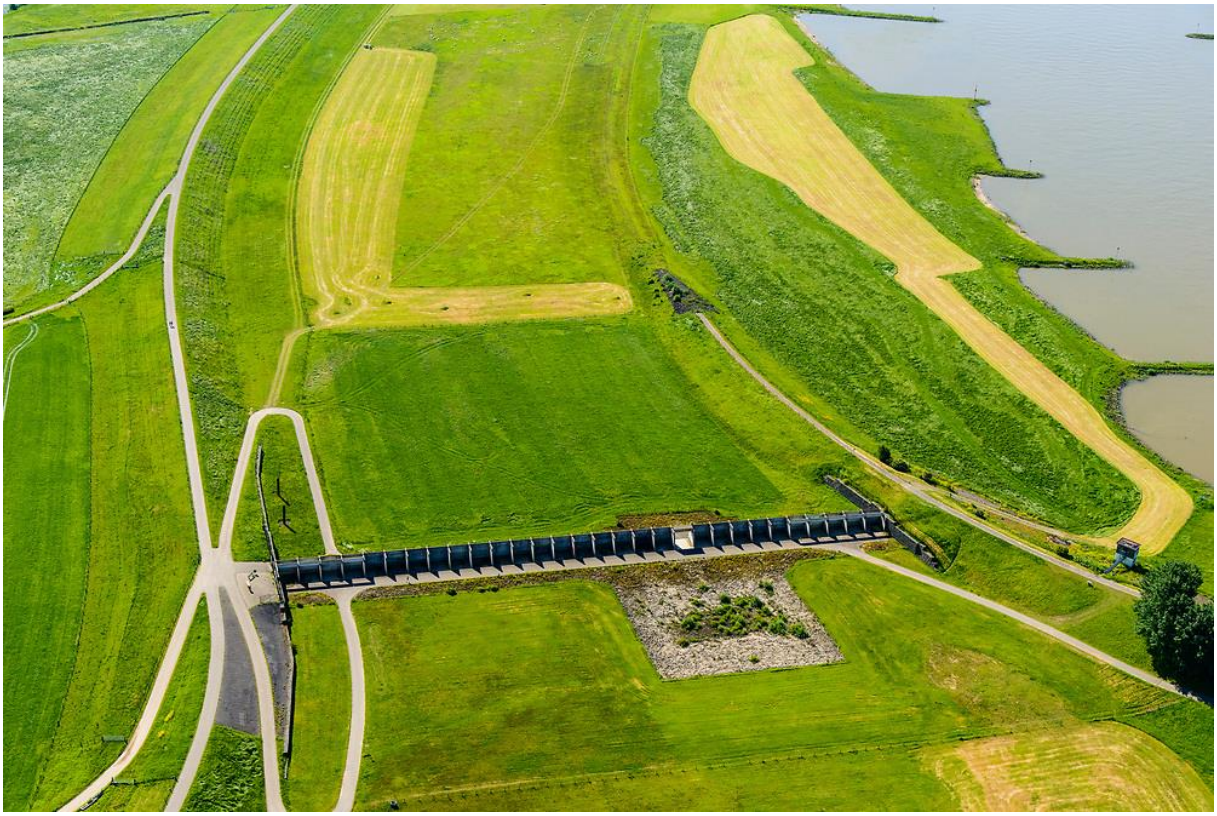

Figure 1 Compound weir in the Hondsbroeksche Pleij flood plain. (Swart, 2019)

Most previous research focused on triangular and/or trapezoidal weirs used in small scale environments to, for example, control irrigation. Research on interaction between individual gates of compound weirs like in Figure 1 is limited. To make optimal use of the flexibility of these structures, interaction between gates and their effects on the stage-discharge relationship should be researched. The results of this can also be used to satisfy other boundary conditions and demands, for example if a certain flow pattern is desired or if one part of the weir is (temporarily) out of use.

The objective of this bachelor thesis is to find stage-discharge relations of a compound weir similar to the one depicted in Figure 1. This is expected to be influenced by transverse (lateral) velocities upstream of the weir due to different weir heights in the gates and thus, different inflow conditions. It is of interest

whether the configuration of the weir has any influence on the discharge coefficients or if these are solely determined by the average weir height. There is improved on previous research on this exact type of weir by Jansen (2020). His research focused on quantifying lateral flow in front of a compound weir and made use of continuity and a balance of forces. This research uses a different approach based on Carnot losses, momentum- and energy conservation. A new model is created and put into practice. Furthermore, flow patterns related to weir configurations are researched. The energy head loss due to the buttresses is not researched.

1.1 Research questions

To address the problems mentioned before, the following research question is be answered: *"How is the flow over a compound weir affected by the configuration of the individual weirs?"*

To formulate an answer to this research question, the following sub-questions are formulated:

i. What is an analytical approach to model a compound weir consisting of multiple gates?
ii. How do different weir configurations affect the discharge coefficient of a compound weir and the lateral flow in front of a compound weir?
iii. Can the discharge coefficient and the flow patterns be predicted from a weir configuration using the previously found analytical model?

1.2 Methods

The following methods are be adapted to be able to answer the sub-questions and finally the research question:

1. Literature study
2. Derivation of an analytical model
3. Experimentation in a flume
4. Validation of the model

In Chapter 2, an analytical approach is used to model flow over a compound weir. In Chapter 3, the experiments in the flume are elaborated on. In Chapter 4, the results of the experiment are discussed, and the model is validated. Chapter 5, 6 and 7 discuss the relevance and significance of the results, draw conclusions, and make recommendations for future research, respectively.

2. Analytical approach to compound weirs

In this chapter, an analytical model is derived to predict water levels and the corresponding discharge coefficients of compound weirs. This is done by studying literature on the subject of (compound) weirs and combining findings and boundary conditions to create the model. Firstly, the geometry is defined and the general weir equations are given. Secondly, the energy, momentum and Carnot equations are given. Then, the discharge coefficient of a perfect weir is discussed and the imperfect flow conditions are modelled using nondimensionalization. Finally, the relevance of backwater curves is discussed.

For future reference, with the word configuration a configuration of the compound weir is indicated. This can be any arbitrary configuration with different weir heights for each gate.

2.1 Classification of weir flow

This section was partially adapted from previous work on the subject by Jansen (2020) and summarized to form a complete view of weirs.

2.1.1 Weir dimensions

As was mentioned in the introduction, the considered weir type is be a sharp-crested weir. Looking at the considered weir in Figure 1, it is clear that the ratio of the weir length and the potential upstream water depth (H/L) exceeds 1.5, making this a sharp-crested weir (Jain, 2001). This allows for neglection of the energy dissipation on the weir (Bos, 1975).

2.1.2 Weir conditions

Two possible weir flow conditions are distinguished: perfect (Figure 2a) and imperfect flow (Figure 2b).

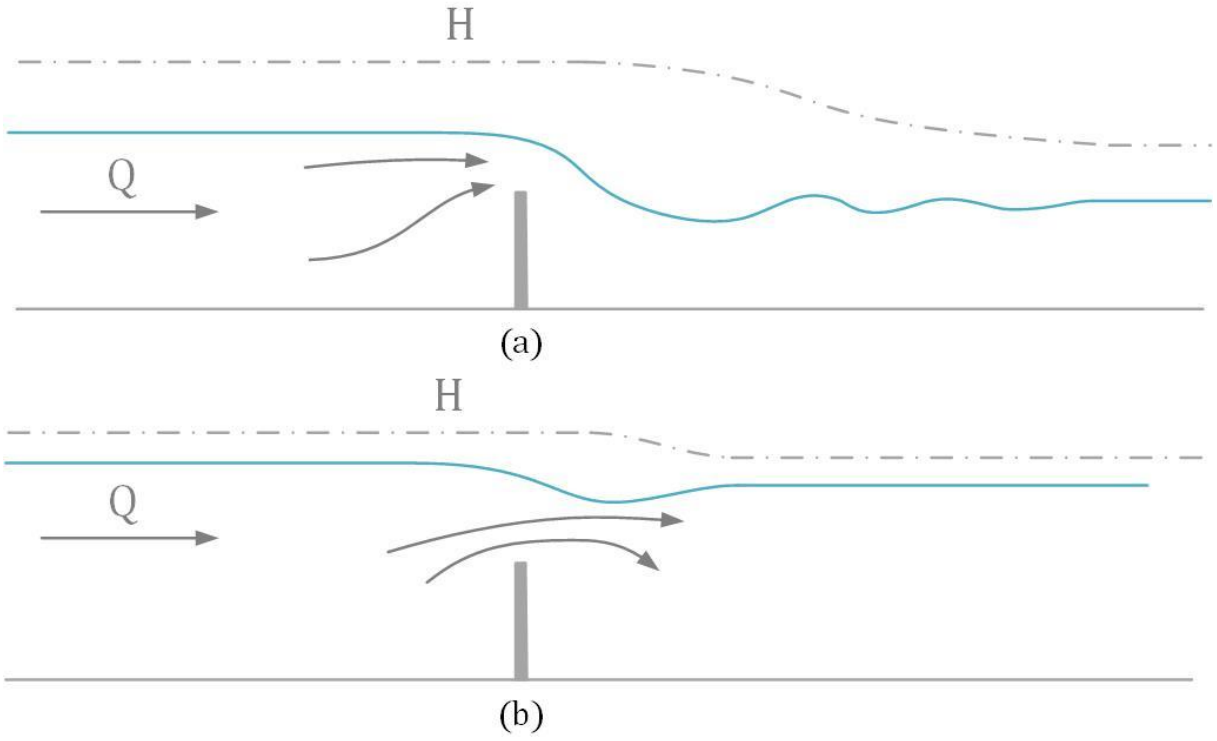

Figure 2 Perfect (a) and imperfect (b) flow conditions over a sharp-crested weir.

For future references, h_0, h_1 and h_2 are the upstream water level, the water level on top of the weir and the downstream water level, respectively. The same applies to the respective energy heads H_0, H_1 and H_2. These definitions are shown in Figure 3.

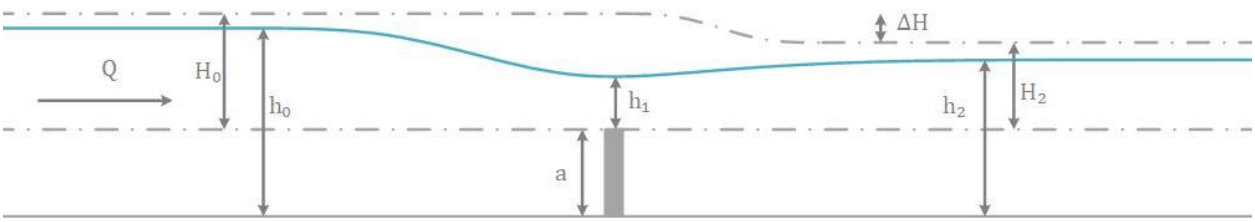

Figure 3 Definitions for the water height and energy head at different points. The image shows imperfect weir conditions. The same definitions apply for perfect weir conditions.

The situation of perfect weir flow (Figure 2a) occurs when the floodplains have not been inundated yet. Flow on top of the weir is (super-)critical in this case and the downstream water level has no influence on the upstream water level.

For perfect weir conditions, relations follow from energy conservation (Bos, 1975):

$$q = C_p \cdot \frac{2}{3} H_0 \sqrt{\frac{2}{3} g H_0} \qquad 2.1$$

In which:

q	the discharge per unit width	$[m^2/s]$
C_p	the discharge coefficient for a perfect weir	$[-]$
g	the gravitational acceleration	$[m/s^2]$

Imperfect weir flow (Figure 2b) occurs when the floodplains have been inundated and the difference between upstream and downstream water level is small. The flow is sub-critical, meaning the downstream water level affects the upstream water level.

For imperfect weir flow, the equation by Mosselman and Struiksma is used (Van Leeuwen, 2006):

$$q = C_i \cdot (h_2 - a) \cdot \sqrt{2g(h_0 - h_2)} \qquad 2.2$$

In which:

C_i	the discharge coefficient for an imperfect weir	$[-]$
a	the weir height	$[m]$

For a sharp crested weir, energy dissipation on top of the weir can be ignored (Bos, 1975) and thus the only energy dissipation is due to expansion loss. Between section 0 and 1, energy conservation is used and between section 1 and 2 momentum conservation is used. For imperfect weir conditions, the energy and momentum equation are respectively (Ali, 2013):

$$h_0 + \frac{q^2}{2gh_0^2} = h_1 + a + \frac{q^2}{2gh_1^2} \qquad 2.3$$

$$\frac{1}{2} g(h_1 + a)^2 + \frac{q^2}{h_1} = \frac{1}{2} g h_2^2 + \frac{q^2}{h_2} \qquad 2.4$$

Instead of using the momentum equation, it is also possible to use Carnot losses to describe the energy loss between section 1 and 2 (Ali, 2013):

$$h_1 + a + \frac{q^2}{2gh_1^2} = h_2 + \frac{q^2}{2gh_2^2} + \frac{1}{2g}\left(\frac{q}{h_1} - \frac{q}{h_2}\right)^2 \qquad 2.5$$

2.2 Discharge coefficients

Discharge coefficients (such as in equations *2.1* and *2.2*) are added to account for the following assumptions:

i. "The height of the water level above the weir is $h = h_1$ and there is no contraction;
ii. velocities over the weir crest are almost horizontal;
iii. the approach velocity head is neglected." (Bos, 1975)

In the case of a compound weir consisting of multiple individual gates, discharge coefficients are unknown. Apart from the assumptions that were listed above, other unknowns are accounted for as well:

- lateral flow in front of the gates
- shape and size of the buttresses between the gates

In this section, it is shown how discharge coefficients can be predicted for both perfect and imperfect flow.

2.2.1 Discharge coefficient of a perfect weir

For a sharp-crested, perfect weir the discharge coefficient is calculated using Rehbock's formulation. It is assumed that the surface tension term is negligible (Ali, 2013; Jain, 2001; Van Leeuwen, 2006).

$$C_p = 0.611 + 0.075\frac{h_0}{a} \qquad 2.6$$

In which:

C_p	the discharge coefficient for a perfect weir	$[-]$
a	the weir height	$[m]$

This discharge coefficient can be used as a starting value for iterations or for a general idea of the weir flow. This coefficient only holds for a singular weir without influences from adjacent weirs. Therefore, it cannot be used in a momentum or energy balance. Jansen (2020) found that the discharge coefficient that is found using Rebhock's formulation cannot be used for any predictions regarding discharge through an individual gate or to predict the upstream water level. Whether the upstream-, weir- or downstream conditions are used as starting condition, the boundary conditions are satisfied.

In this section, proof is presented that the discharge coefficient for the average height of a weir is not the same as the accumulated discharge coefficients for each individual gate. For this derivation, the Rehbock formulation is used. Note that equation *2.6* only holds if there is perfect flow. The arbitrary compound weir that is chosen as an example has the following dimensions for height:

Gate 1	$0.5a$
Gate 2	$0.75a$
Gate 3	$1.5a$
Gate 4	$2a$
Gate 5	$0.25a$

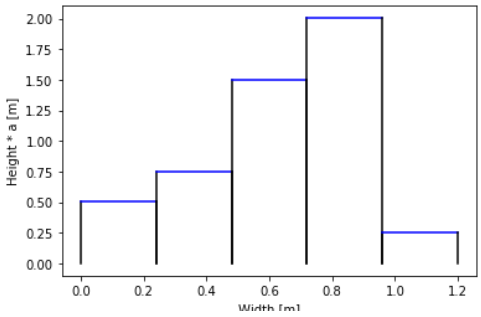

Figure 4 Example weir configuration.

Each gate has the same width. The example weir is shown in Figure 4.

The average height of this weir is a. This means that the discharge coefficient according to Rehbock is the same as equation *2.6*, but with a as the average weir height. If each gate is considered individually, the discharge coefficient becomes:

$$C_p = \frac{1}{5}\sum_{i}^{n}\left(0.611 + 0.075\frac{h_0}{a_i}\right) \qquad 2.7$$

If this is completely worked out, it yields:

$$C_p = \frac{1}{5}\left(0.611 \cdot 5 + 0.075 h_0\left(\frac{1}{0.5a} + \frac{1}{0.75a} + \frac{1}{1.5a} + \frac{1}{2a} + \frac{1}{0.25a}\right)\right) \qquad 2.8$$

$$C_p = 0.611 + 1.7 \cdot 0.075\frac{h_0}{a} \neq 0.611 + 0.075\frac{h_0}{a} \qquad 2.9$$

It is therefore concluded that the discharge coefficient of a compound weir is not necessarily the same when calculated for the average weir height and when calculated for the heights of the individual weirs.

For a compound weir consisting of two gates, the comparison between the two approaches to calculate the discharge coefficient is visualized in Figure 5.

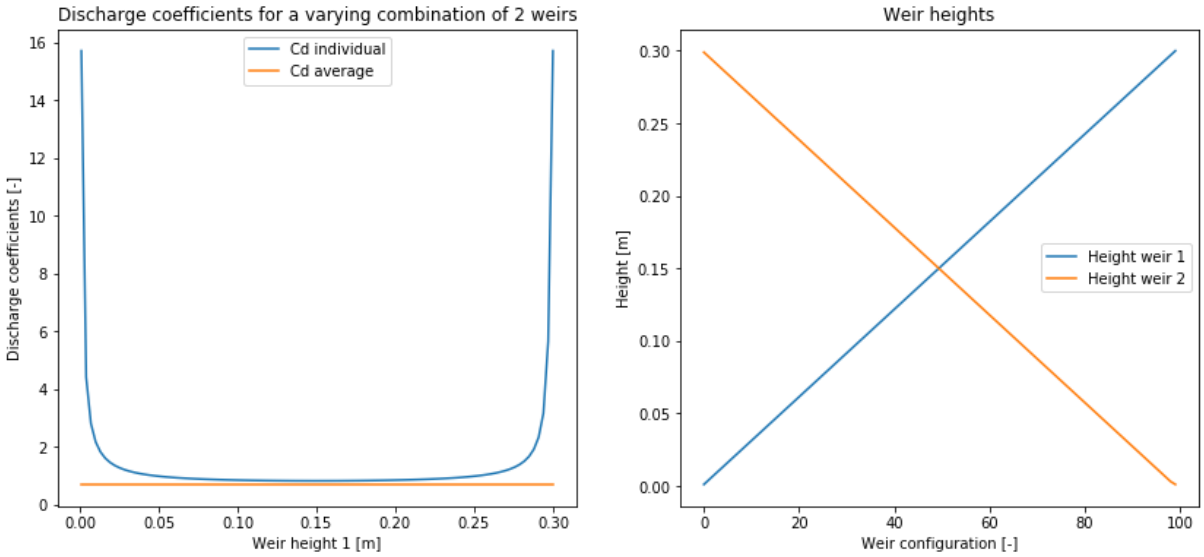

Figure 5 Discharge coefficients (left) for different height combinations (right) of a compound weir that consists of two individual weirs. The discharge coefficients are only the same if the weir heights are equal.

Both the method making use of the individual weir heights and the method making use of the average weir height is used to predict discharge coefficients of perfect weirs.

If the flow conditions are known (for example during an experiment), the discharge coefficient upstream follows directly from the water level and the discharge, using equation *2.1*:

$$C_p = \frac{q}{\frac{2}{3}H_0\sqrt{\frac{2}{3}gH_0}} \qquad 2.10$$

2.2.2 Discharge coefficient of an imperfect weir

The discharge coefficient of an imperfect weir cannot be calculated just by using the weir height and the upstream and downstream water level. Instead, it follows from equation *2.2* once all the parameters and the discharge are known. The next section discusses how all parameters are determined.

2.3 Nondimensional approach

The Froude-number is defined as (Jain, 2001; Battjes & Labeur, 2017):

$$Fr = \frac{U}{\sqrt{gh}} = \frac{q}{h\sqrt{gh}} \qquad 2.11$$

In which:

Fr	the Froude number	$[-]$
U	the flow velocity	$[m/s]$
h	the water depth	$[m]$

To make the calculation of the discharge coefficients for imperfect weir conditions easier, the nondimensional approach is proposed (Ali, 2013). All lengths are nondimensionalized using the critical water depth above the weir. Using $Fr = 1$, the critical depth above the weir is:

$$h_{cr1} = \sqrt[3]{\frac{q^2}{g}} \qquad 2.12$$

Note that the dimension of the critical water depth is meters, so when an equation is nondimensionalized using the critical water depth, attention must be paid to what unit the equation is in and if it should be nondimensionalized using h_{cr1}, h_{cr1}^2 or a higher power.

2.3.1 Nondimensional approach for a single weir

A single weir only has one weir height. The entire discharge flows over this weir and is known in the case of the experiment. It is also assumed that the downstream water level is known. The objective of this section is to find the upstream water level and subsequently the discharge coefficient for an imperfect weir.

For imperfect weirs, the energy (equation *2.3*) and momentum (equation *2.4*) conservation equations become (Ali, 2013):

$$h_0^* + \frac{1}{h_0^{*\,2}} = h_1^* + a^* + \frac{1}{h_1^{*\,2}} \qquad 2.13$$

$$(h_1^* + a^*)^2 + \frac{2}{h_1^*} = h_2^{*\,2} + \frac{2}{h_2^*} \qquad 2.14$$

In which:

h_0^*	nondimensionalized upstream water level	$[-]$
h_1^*	nondimensionalized water level above the weir	$[-]$
h_2^*	nondimensionalized downstream water level	$[-]$

Note that the momentum equation needs to be solved for h_1^*, resulting in a 3rd degree polynomial, yielding three solutions. These solutions need to be checked to find if they are: 1. real, 2. positive and 3. possible. For a group of three solutions, one solution can be identified to be correct.

The energy equation is solved for h_0^*, resulting in another 3rd degree polynomial. The same procedure is applied.

The Carnot losses (equation *2.5*) are rewritten to (Ali, 2013):

$$h_1^* + a^* + \frac{1}{h_1^* h_2^*} = h_2^* + \frac{1}{h_2^{*\,2}} \qquad 2.15$$

This equation is solved for h_1^* resulting in a 2nd degree polynomial. Again, the possibility of each result must be checked.

Now that the nondimensionalized upstream water level h_0^* is found, it can be dimensionalized using equation *2.12* to find the upstream water level. The discharge coefficient can be found using equation *2.2*:

$$C_i = \frac{q}{(h_2 - a) \cdot \sqrt{2g(h_0 - h_2)}} \qquad 2.16$$

Combining discharge coefficients for each individual weir of the compound weir is not possible, so for the weir height a, the average weir height is used.

The following part discusses the interval at which imperfect weir flow is expected to occur.

In the experiment, h_2 is varied to create different upstream effects. It can be varied from a high level (where $h_1 = h_2$) to a lower level (where $h_1 = h_{cr1}$). This is the interval for imperfect weir flow. The highest h_2 provides the highest Froude number and thus the smallest losses. As losses are small for this flow, the minimum Fr_1 can be estimated as (W.S.J. Uijttewaal, personal communication, September 14th, 2021):

$$Fr_1^* = h_1^{*\,-3/2} \cong (h_2^* - a^*)^{-3/2} \qquad 2.17$$

For critical flow, the nondimensionalized h_1 is equal to 1. The momentum equation becomes:

$$(1 + a^*)^2 + 2 = h_{2;cr}^{*\,2} + \frac{2}{h_{2;cr}^*} \qquad 2.18$$

If h_2 is lowered further, the flow becomes perfect. The minimum value of h_2^* is found by solving this equation. It is concluded that the weir height a is the only free parameter (W.S.J. Uijttewaal, personal communication, September 14th, 2021), as the interval at which h_2 is researched depends on the weir height a. $h_{2;max}$ is determined by the experimental constraints or, in the real situation, by downstream constraints.

2.3.2 Nondimensional approach for a compound weir

A compound weir consists of multiple weirs, each with a weir height and an unknown discharge. The upstream water level is unknown as well. The same energy- momentum- and Carnot equations as for a single weir apply for each of the weirs of the compound weir. It is known that the sum of the discharges over each weir should add up to the total discharge. Furthermore, the upstream water level h_0 is the same for each gate. This gives the following boundary conditions:

$$\sum_{i=1}^{n} q_i B_i = Q \qquad 2.19$$

$$h_{0;\,1} = h_{0;\,2} = \ldots = h_{0;\,n} \qquad 2.20$$

There are n unknowns and n boundary conditions, so this system of equations can be solved to find the discharge through each gate.

2.4 Backwater curves

Due to control structures, a new steady state arises if the configuration of the control structures stays the same. For a sub-critical flow, these variations propagate in upstream direction, causing a different steady state of the water height. This effect is described by back water curves. For sub-critical flows, this is an M-curve (Battjes & Labeur, 2017). Due to a build-up of water in front of the weir, an M_1-curve forms. This means that the water rises in front of the weir. This rise propagates upstream. This is visualized in Figure 6.

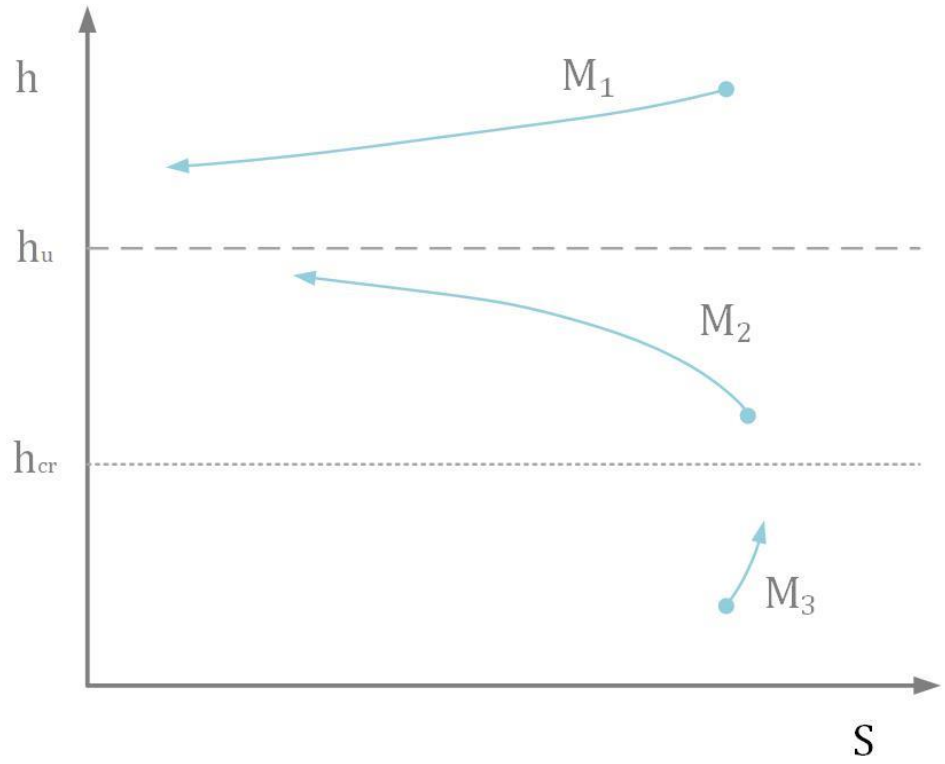

Figure 6 M-backwater curves for subcritical flow. The flow is directed to the right, h_u is the equilibrium depth and h_{cr} is the critical depth.

The slope of the backwater curve is calculated using (Battjes & Labeur, 2017):

$$\frac{dd}{ds} = \frac{i_b - i_f}{1 - Fr^2} \qquad 2.21$$

This is re-written to:

$$\frac{dd}{ds} = i_b \frac{d^3 - d_u^3}{d^3 - d_{cr}^3} \qquad 2.22$$

Different weir heights of adjacent weirs cause different backwater curves. This leads to different water heights in the lateral direction (perpendicular to the flow). Due to these variations, lateral flow occurs. This effect and its importance is investigated in Chapter 4 when data is obtained on flow lines. Induced water level differences on experimental scale are expected to be insignificant when measured with the available equipment. This is because the adaptation length (the length that is affected by the backwater

curve) is inversely proportional to the bed slope (Battjes & Labeur, 2017), causing adaptation length to be of an order of magnitude that is considerably bigger than the length of the experiment.

2.5 Summary analytical model

The relations that are used in the model are summarized in Table 1.

Table 1 Summary of the relations that are used to predict discharge coefficients.

Perfect weir flow Individual weir heights and average weir height	- Rehbock
Imperfect weir flow Individual weir heights and average weir height	- Momentum balance - Carnot losses

Each relation can be approached using the average weir height over the compound weir or using the individual weir heights. These approaches are referred to as the “average” and the “individual” method/approach.

It is researched which of these approaches yields good approximations of the actual discharge coefficients that are researched in the experiment. Predictions are compared to the experimental results. By comparing these, it becomes clear when the biggest deviations from the predictions occur and for which model they occur.

It is expected that turbulence affects the discharge coefficient. Furthermore, it is expected that lateral flow affects the discharge coefficient as well. How the discharge coefficient is affected is researched in the experiment.

3. Compound weir experiment

In this chapter, everything related to the compound weir experiment is discussed. This experiment is needed to collect data in the form of water levels for different weir configurations and to gain insight into the flow patterns. Using this data, the compound weir model can be verified. The insights in flow patterns and lateral flow can be used to add new possible energy head losses related to lateral flow and to research the importance of backwater curves.

Firstly, the experimental setup is discussed to explain the experimental procedure, to identify potential flaws in the data and to identify possible opportunities. After this, interesting weir configurations are identified.

3.1 Experimental setup

The experiment is performed in the Hydraulic Engineering Laboratory at the Delft University of Technology. The "3-m shallow flows flume" is used for the experiment. In this flume, a 1:20 scale model of a compound weir was built. This scale model consists of 12 gates with buttresses and panels in between those buttresses. Panels can be stacked up to 4. Gates allow flow if there is a maximum of 3 panels stacked.

Figure 7 The experimental setup with buttresses and panels. The model consists of 12 gates. Each gate can be configurated individually.

The experiment is set up in the following way. The discharge can be adjusted using a gate on the pipe. The downstream water level can be adjusted with a wooden gate at the end of the flume. The compound weir can be configurated arbitrarily, after which the upstream and downstream water levels are measured using lasers. Even though the downstream water level is set, it must be measured to guarantee maximum precision. Ultimately, the upstream water level is the interesting measure, because the influence of the weir configuration on the upstream water level is of interest. At the upstream end of the flume, a particle dispenser is located. A camera can be mounted above the flume. This mount can be adjusted to have different locations. The geometry of the setup is given in Appendix A.1 and photos are shown in Appendix A.2.

3.1.1 Scaling

The model was built to resemble the prototype near Pannerden using a scale of 1:20. All the exact measurements are shown in Appendix A.1. To summarize, all panels have a height of 5 cm and the buttresses a height of 25 cm, whereas these measurements of the actual structure are 1 m and 5 m (Staatsbosbeheer, 2018), respectively.

When comparing models to the actual situation, dynamic similitude is of importance. This means that significant π-groups should be the same for model and reality. However, this is only possible in the prototype (scale 1:1). The groups that are of relevance in this case are (Elger et al., 2016):

- Froude number
- Reynolds number

Froude similitude and Reynolds similitude should be considered.

The Froude number is defined in equation *2.11*. In case of Froude similarity, the Froude number should be the same for the model and the real situation. This results in the following equation, where m

denotes the model and p denotes the prototype (Queen's University [MECH 241 - Fluid Mechanics I], 2017):

$$Fr_m = \frac{Q_m}{B_m h_m \sqrt{g h_m}} = \frac{Q_p}{B_p h_p \sqrt{g h_p}} = Fr_p \qquad 3.1$$

In which:

Fr_m	the Froude number of the model	$[-]$
Fr_p	the Froude number of the prototype	$[-]$
Q_m	the discharge of the model	$[m^3/s]$
Q_p	the discharge of the prototype	$[m^3/s]$

This results in:

$$Q_m = Q_p \cdot \frac{B_m h_m \sqrt{g h_m}}{B_p h_p \sqrt{g h_p}} \qquad 3.2$$

In conclusion, when the model is geometrically scaled by a factor 20, the discharge should be scaled by a factor $20^{5/2}$. If the same approach is used for equation *2.11*, it is concluded that the flow velocity is scaled by a factor $20^{1/2}$. Using an order of magnitude of 100 m^3/s for the real civil work near Pannerden, the discharge that should be tested in the lab is around 50 l/s, which is feasible in the lab.

The Reynolds number is given by (Jain, 2001; Battjes & Labeur, 2017):

$$Re = \frac{UL}{\nu} \qquad 3.3$$

In which:

Re	the Reynolds number	$[-]$
U	the flow velocity	$[m/s]$
L	the characteristic length	$[m]$
ν	the kinematic viscosity of the fluid	$[m^2/s]$

With the same approach as for the Froude number it is found that the flow velocity should be increased by factor 20 (or the discharge should be decreased by a factor 20). Both of these options are not practical and cannot be achieved in this experiment.

It is concluded that for this experiment only Froude similarity is achievable. However, it is important that the flow is turbulent, even though Reynolds similarity cannot be achieved. Using a kinematic viscosity ν of $1.14 \cdot 10^{-6}$ (Elger et al., 2016), Reynolds number in the experiment is approximately:

$$Re = \frac{QL}{Bh\nu} \cong \frac{50 \cdot 10^{-3} \cdot 10}{3 \cdot 0.15 \cdot 1.14 \cdot 10^{-6}} \cong 9.74 \cdot 10^5 > 10^4 \qquad 3.4$$

This indicates that there is turbulent flow (Elger et al., 2016). Therefore, scale effects are minimal.

3.1.2 Equipment

In this section, each piece of equipment and its purpose are discussed briefly, including its shortcomings if necessary.

Laser

To measure the upstream and downstream water levels, a laser is used. It reflects on a piece of paper that floats on the water when the water level gets sufficiently high (Figure 8). It gives an output in

voltage, which must be converted to a distance. This was done by calibrating the laser with 5 points (Appendix A.3).

The laser is set to perform at 10 Hz. Even though ultimately only one water level is used for computations, a measurement is conducted for an average of 30s and the mean is used to account for outliers and to reduce random error.

The laser measures with a significance of 0.01V. After calibration, it was found that 0.01V translates to 0.2 – 0.3 mm.

Figure 8 The setup for the laser. It only works if the paper reflects the laser, in other words when the water level is high enough.

Discharge
The discharge is set using a control gate on the pipe. This is operated manually, making it hard to precisely use a pre-determined discharge.

The discharge is measured using a flowmeter (Proline Prosonic Flow 91W ultrasonic flowmeter) making use of ultrasound. From experience, the discharge measurements fluctuate around a mean. This means that there is not actually a set discharge. This is most likely due to air bubbles in the pipe or due to pressure variations. Due to this variation, it is hard to calibrate the discharge and create a linear formula to convert the discharge measurements to the right unit. Through testing with Python, it was found that discharge variations of around 0.5 l/s change the discharge coefficient with around 0.005. The flowmeter can be read with a higher precision than this and the mean of the discharge can be estimated well with an estimated significance of 0.1 l/s. For the discharge in the model, the estimated mean value that is read off the flowmeter is be used.

Particle dispenser
At the upstream end of the flume, a particle dispenser is installed. It releases black particles that float on the water. In combination with a camera setup, this can be used for PIV (Particle Image Velocimetry) at a later stage.

Camera
On top of the experiment, a wooden frame is built to hold a camera. This camera can make videos of the experiment, particularly of the black particles floating over the compound weir model. As was mentioned, these videos can be used for PIV. The framerate of the camera is 24 fps, and the size of the video images is 4096 x 2160.

Checkerboard patterns with 1 cm squares are installed on three places on the compound weir to use as calibration distances at a later stage.

3.1.3 Procedure

It is important to keep in mind that the discharge and downstream water level are hard to replicate exactly if they are changed in between measurements. To be able to produce results that can be compared to each other, it is important to keep the downstream water level and the discharge consistent. Therefore, the discharge and downstream water level are set firstly. Then, a configuration in the compound weir model is build. Finally, the measurements are performed: the upstream water level, downstream water level and discharge are measured. Then, another configuration is built, and measurements are performed again. When all configurations have been tested, another downstream water level is chosen, but the discharge stays the same. For each discharge, multiple downstream water levels are experimented on and for each water level all configurations are tested. The procedure is visualized in Figure 9.

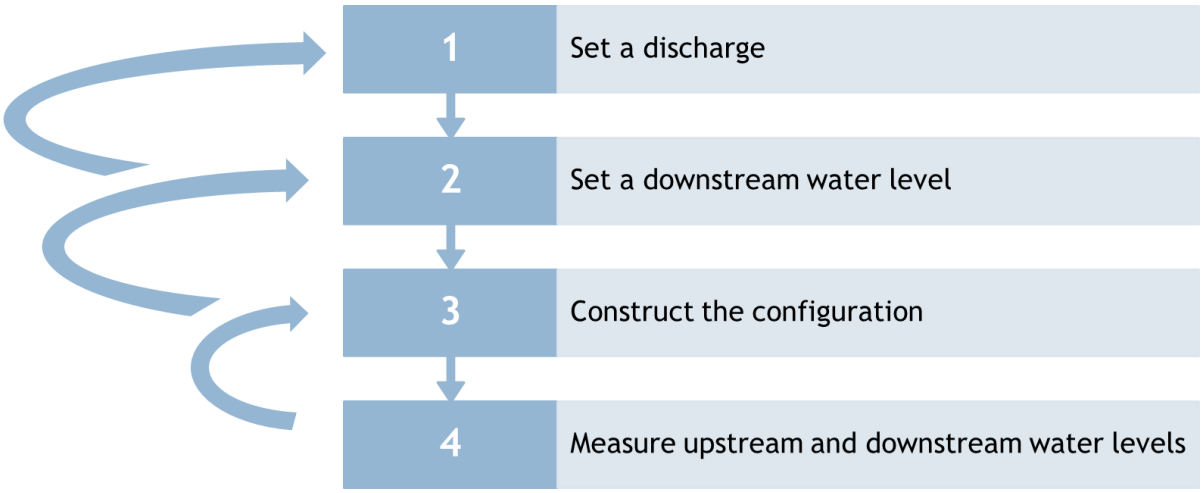

Figure 9 Schematization of the experimental procedure.

Apart from these measurements, there is room to videorecord a handful of weir configurations to later use for Particle Image Velocimetry.

3.2 Identifying interesting weir configurations

This section firstly identifies weir configurations that are tested herein. For each of these configurations, predictions are made regarding the discharge coefficient using the analytical model described in Chapter 2. These predictions are made in the next chapter.

Several weir configurations are identified that induce lateral flow. Each of these configurations is tested with a varying discharge and varying downstream conditions to research the effects on and of lateral flow. Configurations are chosen based on a few criteria:

- Will the configuration induce lateral flow? As mentioned, lateral flow is expected to influence head losses and the amount of contraction on top of the weir (and thus the flow velocity).
- Does lateral flow happen over a big distance? It is of interest whether the distance over which lateral flow happens affects the discharge coefficient or flow velocity on the weir in any way.
- How and where does the most contraction happen? Contraction on top of a weir reduces the cross-section through which the most water flows. Contraction is paired with higher flow velocities, so bigger energy losses are expected.
- Do instant or gradual weir height changes have an impact? It is expected that a gradual change induces a smaller amount of lateral flow, because more water can flow over the medium high transition from a low to a high weir height. This is expected to affect the discharge coefficient.

The weir configurations that are used in the experiment are shown in Figure 10 and Appendix B.1. The justification of each configuration is done in Appendix B.2.

Finally, a handful of these configurations needs to be selected for PIV. To produce results that can be compared, it would be best to use weir configuration with the same average height. In this way, actual qualitative comparisons can be done between the different configurations. Configurations that are expected to show different behaviour are configuration 5, 6 and 7. Of these configurations, 5 represents the alternate switching between weir heights, 6 represents a sudden change of weir heights and 7 represents a gradual change of weir heights.

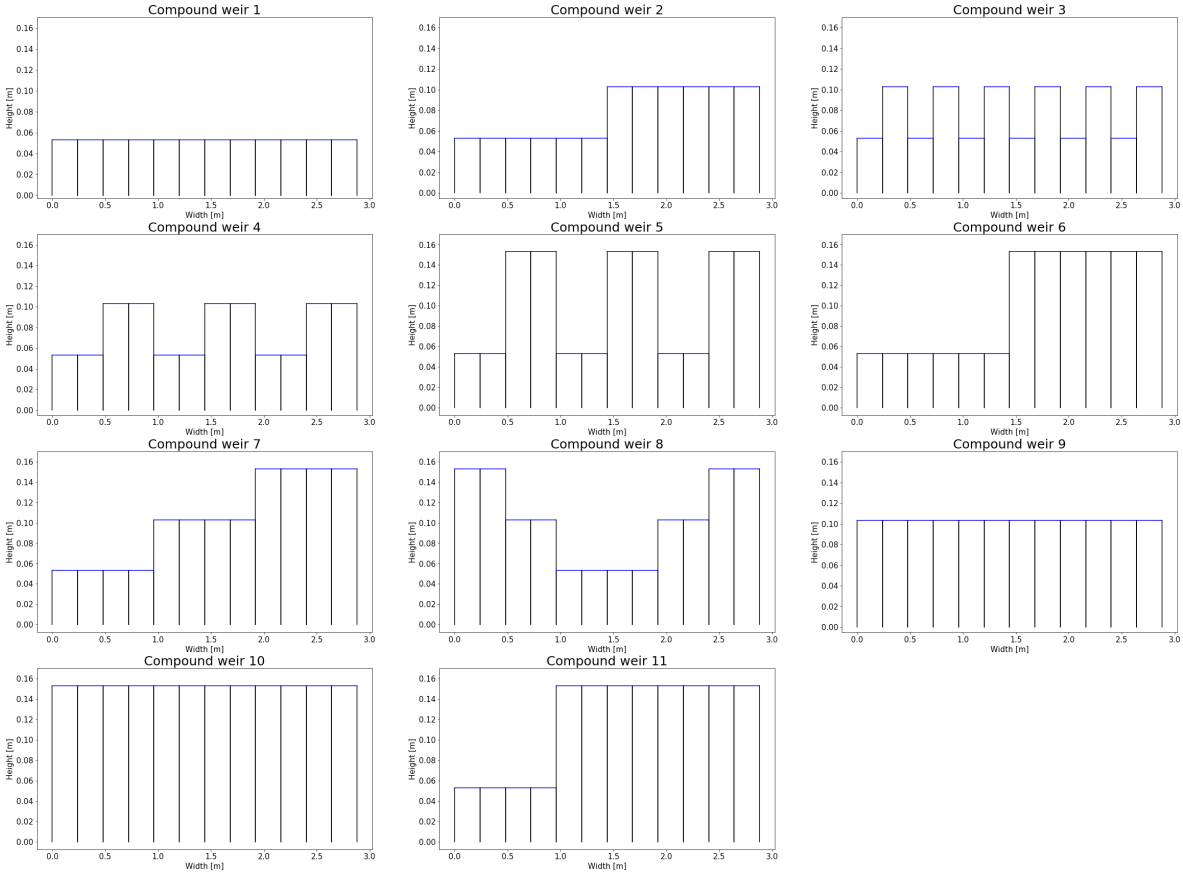

Figure 10 Weir configurations that are experimented on.

4. Model validation

In this chapter, the experiment results are presented firstly. Then, the model as described in Chapter 2 is validated. Finally, PIV is used to create plots that provide more insight into the behaviour of flow over a compound weir.

The discharge coefficients that where found are shown in Figure 11.

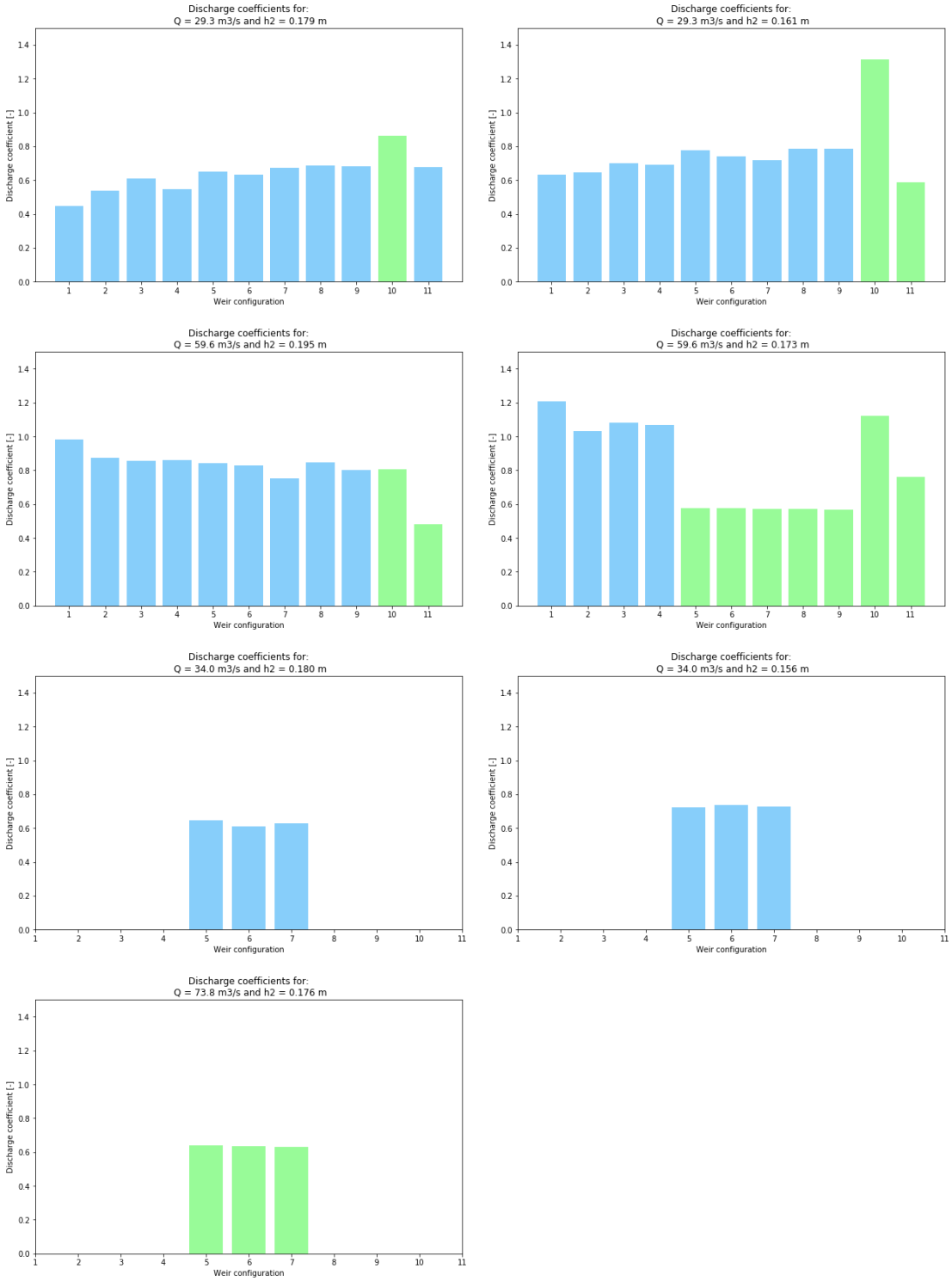

Figure 11 The discharge coefficients that were found in the experiment. Blue indicates imperfect weir flow and green indicates perfect weir flow. Each graph represents a different discharge with a different downstream water height. The data in the bottom three graphs was collected alongside videos to perform PIV.

A brief recap of the experiment is presented in Appendix C. The data that was collected is shown in Appendix D.1. As discussed, nine videos were made. Of these nine videos, three videos turned out to be well suited for PIV.

Configurations 2-4 and 5-9 have the same average weir height. This means that these configurations are directly comparable.

It can be concluded from Figure 11 that discharge coefficients for different configurations show varying behaviour for perfect and imperfect weir conditions. It seems that if the average height of the weir is the same, the discharge coefficients for perfect flow are very similar. It follows from the top two graphs that the discharge coefficients of imperfect weirs do vary. The discharge coefficient varies by around 10-20% for each configuration, indicating that the configuration does influence the discharge coefficient.

Some of the discharge coefficients that follow directly from the measurements exceed 1. This is discussed in the next chapter.

Bar plots of the measurements with every model prediction are shown in Appendix D.2. Scatterplots are shown in Appendix D.3. The scatterplots belonging to configuration 7 are shown in Figure 12.

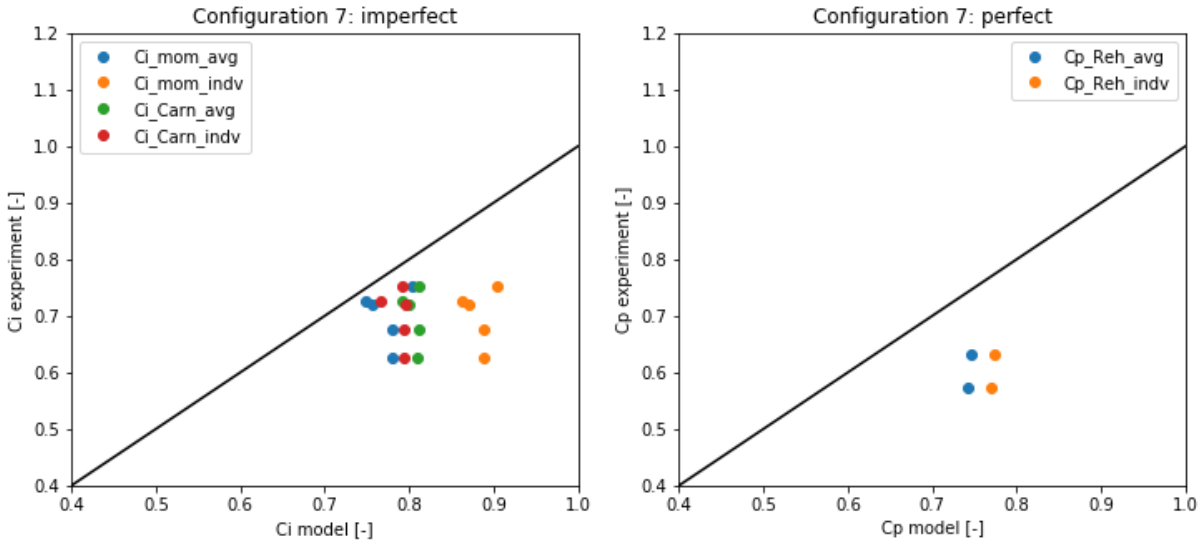

Figure 12 Scatterplots corresponding to configuration 7. The modelled discharge coefficients are displayed on the x-axis and the discharge coefficients found in the experiment are displayed on the y-axis. The black line shows the ideal condition in which the modelled and experimental discharge coefficients are the same.

It can be concluded from the scatterplots in Appendix D.3 that there is no standard factor by which the models differ from the real situation. This means that there is no factor that can be used to calibrate the model directly. The models predict the most accurate values for higher average weir heights. For an average weir height of 7.5 cm (i.e., configurations 2-4), the analytical model consistently predicts discharge coefficients that are too high or too low by a considerable amount. For these configurations, no correlation between the predicted and the actual discharge coefficients can be proven. The predictions resemble the reality more closely for an average weir height of 10 cm (i.e., configurations 5-9), though predictions are often too high.

For imperfect flow, it differs which model has the most accurate prediction. It can be concluded that the model using the individual weir approach with the momentum equation is the least accurate. This is surprising because the weir that this model uses closely resembles the real weir. It is expected that this result is due to the model not incorporating inter-weir-effects. When the weir in a single gate is

lower, the discharge through this gate rises fast due to the quadratic and square terms in equation *2.3* and *2.4*. In reality, this rise is slower due to inter-weir-effects. Therefore, the analytically modelled discharge coefficient using this method is too high. The Carnot model is often more accurate than the momentum model. This can be attributed to the fact that the momentum approach only uses energy head loss of flow velocities. Most of the models have reasonable predictions for the higher average weir heights, except for the individual momentum approach.

For perfect flow, the model using the average weir height seems to be more accurate than the individual approach. The predicted values of the discharge coefficient are too high for most weir configurations, with the average approach consistently being a little lower than the individual approach. The model predictions are too high by around 0.15 (25%) in most cases.

PIV (Thielicke & Sonntag, 2021) was performed on three configurations (Figure 10: configuration 5, 6 and 7) with imperfect flow. This was done to gain additional insight in the flow patterns over the compound weir. The corresponding data is shown in Appendix D.1.

The PIV procedure and settings are discussed in Appendix D.4. The results are shown in Appendix D.5. The streamlines were found by creating an image of the mean pixel values,. These are also shown in Appendix D.5. Due to the small elevation and darker colour at the location of the weir, numerical values for the flow velocity on top of the weir could not be found with PIV. Therefore, the PIV results are used qualitatively. The flow magnitudes and streamlines of configuration 5, 6 and 7 are shown in Figure 13.

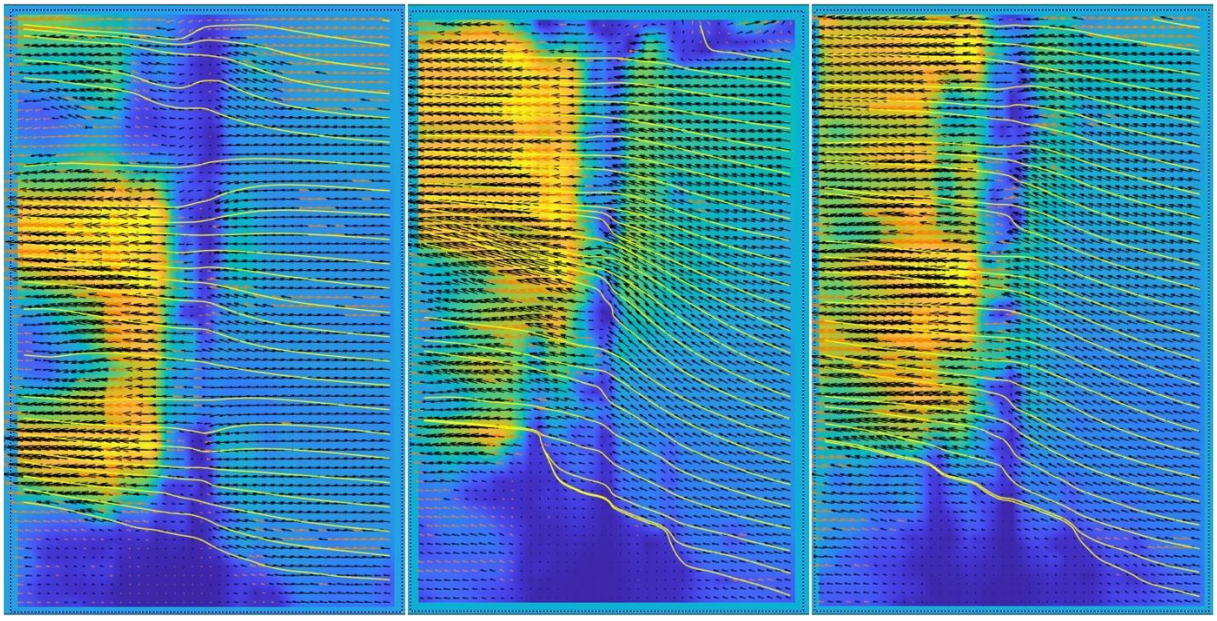

Figure 13 PIV results of configuration 5, 6 and 7 respectively. The colour indicates the qualitative velocity magnitude, vectors indicate the flow direction, and the streamlines are displayed as yellow lines.

It can be concluded from the streamlines that when the transition from a low to high weir height is gradual (configuration 7), and the angle at which the flow hits the weir is smaller than when the transition is sudden (configuration 6). This effect is the biggest for the gates in the middle of the weir and seems to get smaller for the gates located at the sides of the flume. It can also be seen that the lateral flow starts well downstream of the weir (see Appendix D.5 for the full images). For configuration 5, lateral flow starts much closer to the weir. Due to the weir configuration, water travels less far (in lateral direction) from a gate with a bigger weir height to a gate with a smaller weir height.

It can be concluded from the PIV results that lateral flow commences further upstream when a greater lateral distance is to be travelled.

Finally, as was discussed in Chapter 2.4, it can be concluded that the importance of backwater curves is small. In the figures in Appendix D.5, at the location where flow enters the image (right), the streamlines are almost parallel with the flume. Backwater curves work over a length scale that well exceeds the 2-3m in the image (Battjes & Labeur, 2017), so the influence of backwater curves can be neglected.

5. Discussion

In this chapter, the significance of the results is discussed. Firstly, the measurement error of the experiment is assessed. Secondly, unexpected results are discussed and an explanation for these results is given. Finally, additional energy losses are identified. These energy losses affected the results and could be an explanation on why certain discharge coefficients turned out too low.

5.1 Measurement error

To give a final interpretation of the results, the measurement error must be discussed to be able to judge how significant certain differences in discharge coefficient for configurations are. Firstly, the measurements error is discussed. Then, the effects of a hydraulic jump on the measured downstream water level are touched upon.

The error of the laser measurements is divided into two parts: the calibration (systematic error) and the output values while measuring (random error). As the discharge coefficient is dimensionless, so are the errors that are calculated.

The systematic error was minimized by calibrating the laser using 5 points and fitting the conversion formula to these points. To give an indication of the quality of the calibration, the correlation coefficient is calculated to be $|r| = 0.9999$ for both lasers. This does not lead to a significant error in the measurements.

The accuracy of the laser outputs was 0.01 V, corresponding to around 0.025 cm. The standard deviation of the water level measurements is calculated to be 0.015 V. This is reduced by taking the mean. Measurements were each done for at least 20 seconds at 10 Hz, adding up to 200 measurements. This reduced the standard deviation by a factor $\sqrt{200}$. This all adds up to an error of O(-3) cm or O(-5) m. If the upstream water level is risen by this amount and the downstream water levels is lowered by this amount (worst case scenario), this attributes to a change in discharge coefficient of imperfect weir conditions of up to 0.008 for normal discharge coefficient values and if the coefficient exceeds 1 it can make a difference of up to 0.033. For perfect weir conditions, this change amounts to a maximum of 0.002.

As was said in Chapter 3, the error corresponding to the discharge measurement attributes around 0.005 to the error in the discharge coefficient. This is added to the previously found error to get the total measurement error.

A hydraulic jump is the result of super-critical flow “jumping” back to sub-critical flow conditions. This is paired with energy losses, but more importantly, a lot of turbulence and possible surface fluctuations. Turbulence and surface fluctuations affect the local water level. If a steady state arises in which there are no surface fluctuations that differ in time, but there are some local elevations, this could give invalid measurements downstream of the weir. If the surface fluctuations are not in a steady state, the use of the mean water level should account for the fact that the local water level is alternately increased and decreased by these fluctuations. This does not affect the discharge coefficients, because in the case of a hydraulic jump (perfect weir flow), only upstream conditions are used for the calculation of the discharge coefficient.

5.2 Unexpected results

Firstly, the results that were not according to expectations are summarized:

On multiple occasions, the discharge coefficients were measured to be higher than 1 (Figure 11) by 10% to 30%, which is physically impossible. This happened for configuration 1-4 for a case of imperfect flow

and for configuration 10 for two cases of perfect flow. Configuration 1 has another case of imperfect flow where its discharge coefficient is very close to 1.

In the case of imperfect flow, the upstream water level exceeds the downstream water level, which should mean that the coefficient of discharge cannot be higher than 1. The upstream and downstream water levels lie very close, meaning that there is hardly any loss of energy head. The reason that the calculated discharge coefficients are higher than 1 in this case, could be due to the definition that is used for the discharge coefficient (equation *2.10* and equation *2.16*). This definition is meant to be used for a normal weir. In this case, there is no unambiguous weir height, so the average weir height was used. This could be the reason for the discharge coefficients being higher than 1.

The above explanation does not apply to configuration 1 and 10 if the discharge coefficients are higher than 1, because these configurations have a uniform weir height. It is possible that there were errors in reading the discharge measurements, leading to a wrong discharge for calculation.

5.3 Additional energy losses

From the results of the experiment, it became apparent that the predicted discharge coefficients were too high compared to the measured ones in most cases. In this section, additional energy head losses are identified. These losses were left out of the model but they did affect the measurements.

Energy head losses due to contraction and expansion were mostly unused in the model, except for Carnot losses. Carnot losses were used for one model, but these were limited to expansion losses.

Contraction losses occur in the horizontal plane due to the buttresses being immovable obstacles and the water having to move around them. Due to the buttresses, the effective width of the cross section is lowered. Contraction is also expected to occur due to horizontal flow, but this is not supported by the data. Vertical contraction occurs before the weir, which also comes with contraction losses.

Besides energy losses due to contraction and expansion, there are energy losses due to friction. This was neglected in the model. The flume is made with a glass surface and smooth walls, resulting in a small amount of friction.

Finally, the model did not incorporate any energy losses or gains due to viscous effects, turbulence, or surface tension. The flow experiences head loss due to turbulence. Furthermore, the surface tension term in the Rhebok equation was ignored. Adding this term would lead to a higher discharge coefficient (Van Leeuwen, 2006). There could also be head gains associated with surface tension on top of the weir, due to water being pulled down over the weir by adjacent water (W.S.J. Uijttewaal, personal communication, October 7th, 2021).

6. Conclusion

The goal of this thesis was to find the relations between different weir configurations of the compound weir and the respective discharge coefficients. Analytical models were created and validated using experimental data. Two analytical models were created to predict discharge coefficients: one using momentum- and energy conservation and one using Carnot losses and energy conservation. The experiment was set up in a 3-meter-wide flume in which a scale model of the control structure near Pannerden was built.

PIV (Particle Image Velocimetry) was used to find that the distance from the weir at which lateral flow commences correlates with the weir configuration. If the water must travel over a higher lateral distance (for example from one side of the channel to the other side), this flow commences sooner and hits the weir at an increased angle. Also, if the transition between the weir height of different gates is gradual, the angle at which the flow hits the weir is smaller than for a sudden change. It was also proven that backwater curves are not of importance for this system.

6.1 Perfect weir conditions

The discharge coefficient under perfect weir conditions is somewhat affected by the weir configurations, but mostly by the average weir height. For each but one configuration with different individual weir heights but the same average weir height, the variation of the discharge coefficient lies within the measurement error, which was determined to be 0.007 (or 1%). The maximum deviation was 0.011 (or 1.9%), which is significant but not big. The configuration for which this was the case was a uniform weir height, leading to the following conclusion: the discharge coefficient is a little lower for a uniform weir height than for differing configurations with the same average weir height. This is not in line with the hypothesis, which stated that additional contraction was expected resulting in a lower discharge coefficient if lateral flow occurs (due to different weir heights of adjacent weirs).

For perfect weir conditions, the Rehbock model based on the average weir height performs better than the model based on the individual weir height. The perfect weir flow model was only tested with average weir heights of 10 cm and 15 cm. Both models performed well for 10 cm but did not for 15 cm. The models consistently predicted values that were 20 – 35% too high.

6.2 Imperfect weir conditions

Under imperfect weir conditions, the discharge coefficients varied significantly for different weir configurations with the same average height. The discharge coefficients for the same average weir height vary as much as 0.096 (or 13%) under a significance of 0.013 – 0.038 (or 1.7 – 5.1%). There is no unambiguous indication that one of the tested configurations has a higher or lower discharge coefficient than the rest of the configurations, as it varies which configurations has a relatively higher or lower coefficient for different flow conditions.

The models that were created perform well under imperfect weir conditions for higher average weir heights (10 cm). They do not perform well for lower average weir heights (7.5 cm). For the latter, the predictions were scattered and not in line with the experimental data. For an average weir height of 10 cm, the models consistently predict discharge coefficients that are too high. This is attributed to the fact that contraction- and friction losses were not incorporated in the model as well as losses due to turbulent effects and possible gains due to surface tension effects.

For imperfect conditions, the least performing model is the momentum model based on the individual weir heights. The other models performed well for an average weir height of 10 cm, estimating the discharge coefficient within a range of at least 30%, but with better accuracy (within 20%) in most cases.

7. Recommendations

From this research it has become clear that the discharge coefficient of an imperfect compound weir is affected by its configuration. A lot of configurations were tested with a limited number of different conditions. No unambiguous result were found on the effects that configurations have on the discharge coefficient. It is recommended that in further research more attention is paid to certain configurations, for example gradual and instant transitions of weir heights. These should then be tested under an increased number of flow conditions.

Research should be done into the way that the discharge coefficient of a compound weir was defined for both the experimental and the analytical models. For both perfect and imperfect flow, the weir height had to be subtracted from the water level to get the energy head. An assumption was made that in this case the average weir height could be used. The implications of this remain unclear and should be researched.

The models that were created (for the configurations for which they worked) should be expanded with more forms of energy loss, among which both horizontal and vertical contraction losses and friction losses. A quantitative and zoomed in PIV should be performed to get the best possible insights in the horizontal contraction. The weir base should be another colour or another solution should be found to perform quantitative PIV on this part of the flume.

References

Ali, S. (2013, August). *Flow over weir-like obstacles*. Doctoral thesis: TU Delft. https://doi.org/10.4233/uuid:b9c67923-a84a-47b0-8c0f-6d873ffd1d85

Battjes, J. A., & Labeur, R. J. (2017). *Unsteady Flow in Open Channels* (1st ed.). Cambridge University Press.

Bos, M. G. (1976). *Discharge Measurement Structures* (1st ed.). International Institute for Land Reclamation and Improvement. https://edepot.wur.nl/333324

Elger, D. F., Crowe, C. T., LeBret, B. A., & Roberson, J. A. (2016). *Engineering Fluid Mechanics* (11th ed.). Wiley.

Jain, S. C. (2001). *Open-Channel Flow* (Online ed.). Wiley.

Jansen, M. D. M. (2020, July). *Compound weirs*. Bachelor thesis: TU Delft.

Piratheepan, M., Winston, N. E. F., & Pathirana, K. P. P. (2006). Discharge Measurements in Open Channels using Compound Sharp-Crested Weirs. *Engineer: Journal of the Institution of Engineers, Sri Lanka*, *40*(3), 31–38. https://doi.org/10.4038/engineer.v40i3.7144

Queen's University [MECH 241 - Fluid Mechanics I]. (2017, May 9). *Froude Number Scaling* [Video]. YouTube. https://www.youtube.com/watch?v=1V2ZVha9qTU

Rijkswaterstaat. (2021, September 17). *Pannerdensch Kanaal: waterhuishouding en rivierbeheer*. https://www.rijkswaterstaat.nl/water/projectenoverzicht/pannerdensch-kanaal-waterhuishouding

Staatsbosbeheer. (20–02-18). *Regelwerk Pannerden - Rijnwaardense Uiterwaarden*. Rijnwaardense Uiterwaarden. http://www.rijnwaardenseuiterwaarden.nl/pages/regelwerk-pannerden.html

Swart, S. (2019, May 29). *Luchtfoto Nederrijn Hondsbroeksche Pleij* [Photo]. https://siebeswart.photoshelter.com/image/I0000CsUyTYNIyyA

Thielicke, W., & Sonntag, R. (2021). Particle Image Velocimetry for MATLAB: Accuracy and enhanced algorithms in PIVlab. Journal of Open Research Software, 9. Ubiquity Press, Ltd. Retrieved from https://doi.org/10.5334%2Fjors.334

van Leeuwen, K. C. (2006, October). *Modeling of submerged groynes in 1D hydraulic computations*. Master thesis: University of Twente. http://purl.utwente.nl/essays/57350

Appendix A: Experimental setup

A.1 Geometry

Component		Size [cm]
Step	Height	0.35
	Length	15
Buttress	Height	25
	Length	10-15
	Thickness	1.8
Panels	Height	5.0
	Length	24
	Thickness	0.5

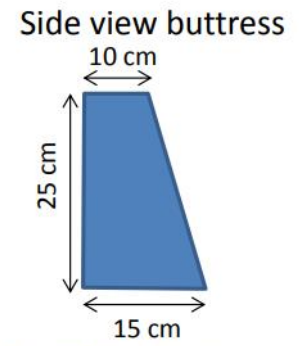

Figure 11: Buttress dimensions as seen from the side.

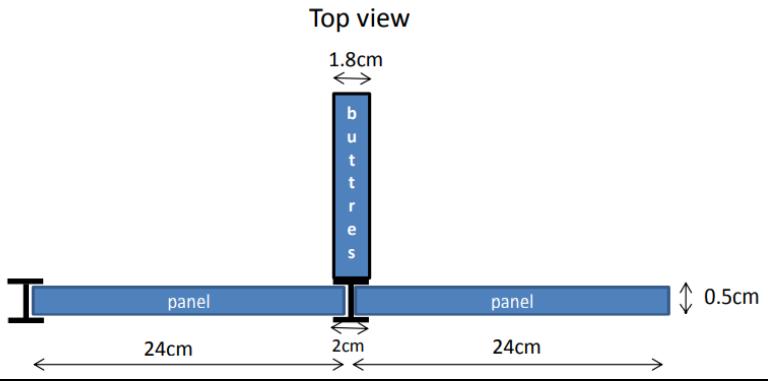

A.2 Pictures of the setup

Figure 14 The flowmeter. It is connected to both the pipe and the computer. Discharge data was collected by reading it directly off the flowmeter.

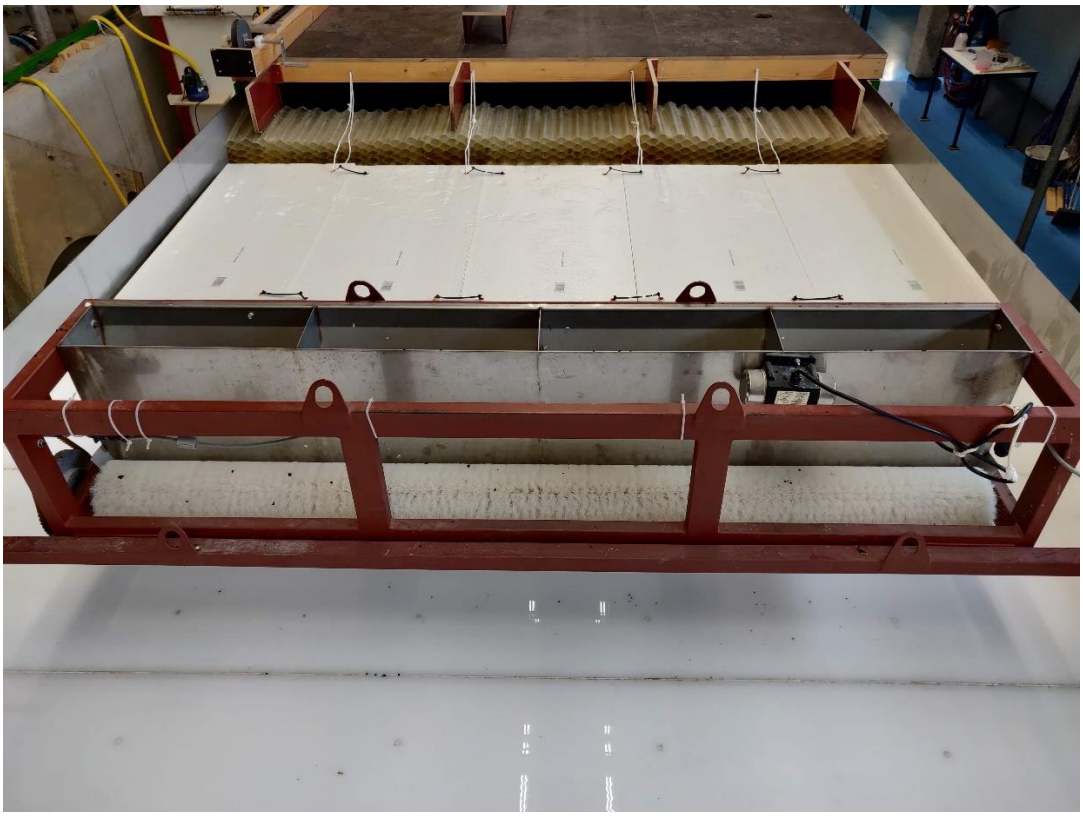

Figure 15 Particle dispenser. It dispenses small black particles.

Figure 16 Gate to set the downstream water level.

Figure 17 The buttresses and the gates with a super critical flow.

Figure 18 Setup to measure the water levels. It consists of a laser that is reflected by a piece of paper floating on the water.

A.3 Laser configuration

The laser was configurated using 5 objects of known heights. It was known beforehand that the voltage is linearly converted to distance. The following measurements were done for calibration:

Table 2 Configuration points of the downstream laser.

h_2 (cm)	U (V)
9.45	8.09
11.83	7.13
14.18	6.19
9.23	8.19
12.83	6.76

Table 3 Configuration points of the upstream laser.

h_0 (cm)	U (V)
9.45	7.91
11.83	6.96
14.18	6.01
9.23	7.98
12.83	6.54

The fitting of linear function is visualized in the following figures:

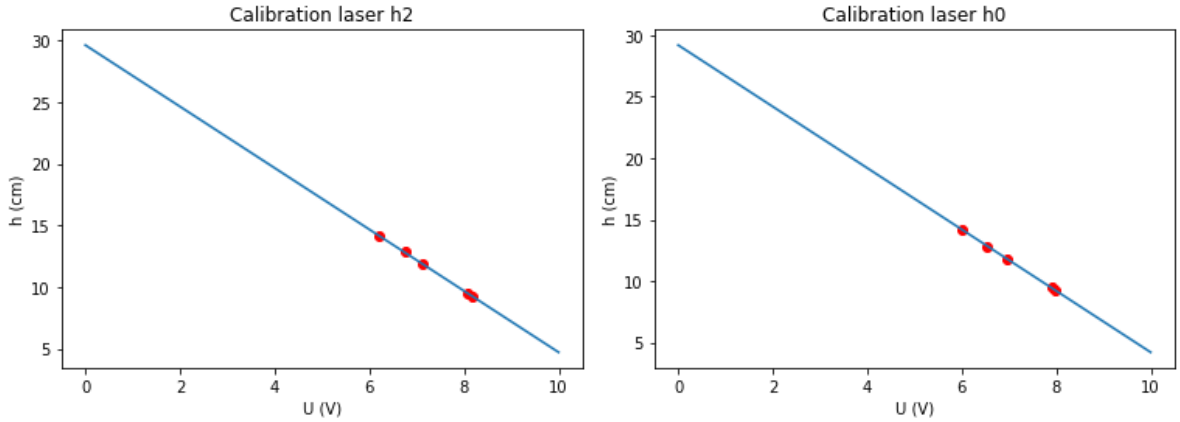

Figure 19 Visualization of the calibration of the lasers.

Using a fitted line through 5 points instead of through 2 points decreases the error. Both calibrations turned out to have correlation coefficients of $|r| = 0.9999$.

Appendix B: Compound weir configurations

B.1 Configurations

Figure 20 The weir configurations on which experiments were conducted.

B.2 Justification of each weir configuration

Table 4 The weir configurations on which experiments were conducted. Each configuration has an explanation as to why this configuration was chosen.

1	Configuration 1 consists entirely of weirs with the same height. It can be used as a reference to the situation in which no lateral flow occurs (contraction can occur due to the buttresses, but this walls outside of the scope of this thesis).
2	In configuration 2, a sudden change in weir height is used from 5 to 10 cm. This is done to research the effects of a sudden weir height change on lateral flow and the discharge coefficient. A weir height of 5 and 10 cm is used because the downstream water level can be set significantly higher than this, so the weir is completely submerged.
3	Configuration 3 makes use of alternately switching weir heights of 5 and 10 cm. This is of interest because in this configuration, lateral flow does occur but not over a large distance, because most water that travels to another gate will only have to travel half a gate to one gate. Due to lateral flow happening in both directions, contraction will happen above the weirs with the lower weir height.
4	Configuration 4 is almost the same as configuration 3 but makes use of larger intervals of the higher and lower weir heights. It is interesting because of the same reasons, but the lateral flow happens over a somewhat larger distance.
5	Configuration 5 is interesting because of the same reason as configuration 4, but the 10 cm weir heights are increased to 15 cm. This is done to increase the amount of lateral flow towards the 5 cm weirs. This is expected to increase the amount of contraction.
6	Configuration 6 is interesting because of the same reason as configuration 2. There will be even more lateral flow and this flow must travel over a large distance.
7	Configuration 7 is used to research the influence that a gradual instead of a sudden change in weir height has on the discharge coefficient. It is expected that lateral flow must travel over a smaller distance.
8	Configuration 8 is used to research whether more contraction occurs when water is guided to the middle of the compound weir by having bigger weir heights on the sides and lower weir heights in the middle. It is expected that contraction will occur.
9	Configuration 9 consists entirely of weirs with the same height. It can be used as a reference to the situation in which no lateral flow occurs.
10	Configuration 10 consists entirely of weirs with the same height. It can be used as a reference to the situation in which no lateral flow occurs.
11	Configuration 11 is relatively less comparable to other configurations. It was included because it is of interested how to discharge coefficient behaves when the average height does not change a lot, but one of the gates is almost all the way open. This will make most of the discharge flow through this gate, so a lot of contraction is expected.

The average heights are the same for configurations 2-4 (7.5 cm) and for configurations 5-9 (10 cm).

Appendix C: Experiment recap

A week was allotted to perform the experiment. Each day is discussed briefly.

1. The first day was used for measuring and calibrating the equipment. The model had not been finished so this needed some work too.
2. The second day was used to perform the first measurements. Due to some difficulties with the model and with starting the experiment, fewer measurements were done than expected. In the end, all configurations were experimented on with one discharge and one downstream water level. It turned out that the data could not be used, because the file that it was written to used commas both as a delimiter and as a separator between values.
3. On the third day, a start with the actual measurements was made. The model still did not cooperate, so experimenting started at noon. On this day, one discharge and two downstream water levels were done.
4. The fourth day was a replication of the third day. Again, one discharge and two downstream water levels were done. The day ended with setting up for PIV on the next day.
5. PIV was planned on the fifth and last day. It proved to take some time before the PIV could be started with. There was no lab assistant present, which is why it was tried to set up everything on the previous day. A lot of extra preparations were necessary. The lab had to be darkened. After this, the camera had to be set up and everything on the setup had to be made in check for filming. Filming started at around 13h. Measurements had to be done as well. In the end, three configurations were filmed with two discharges. The first discharge was filmed with two different downstream water levels and the second discharge was filmed with one downstream water level due to lack of time and a complication with the particle dispenser which accidentally got wet and lost some of its functionality. A consequence of this was that particles got more clustered and less particles where dispensed as a whole.

Appendix D: Experiment results

The data is shown in the following way. For each measurement set, the discharge, upstream water level and downstream water level were measured. It is pretended that the discharge and downstream water level are known beforehand, so the data is represented by just the upstream water level. For the discharge, an average value is used. The different downstream water levels are represented by h2,i and h2,ii. An overview of the data that was collected is shown in Table 5.

Table 5 Representation of the data that was obtained through the experiment. Blue indicates that there are measurements and that there is imperfect flow. Green indicates that there are measurements and that there is perfect flow. Yellow indicates a case where there is doubt whether the flow was perfect or imperfect. Red indicates missing or faulty data. A dash indicates that it was chosen not to do measurements for certain data because it was not possible to do PIV for all the weir configurations.

Discharge [l/s]	Q = 29.3		Q = 59.6		Q = 34.0		Q = 73.8	Q = 40.3
Weir configuration	h2,i	h2,ii	h2,i	h2,ii	h2,i	h2,ii		
1					-	-	-	
2					-	-	-	
3					-	-	-	
4					-	-	-	
5								
6								
7								
8					-	-	-	
9					-	-	-	
10					-	-	-	
11					-	-	-	

D.1 Data

For each discharge and downstream water level, a different table is used. Each table contains information on the upstream and downstream water levels, the discharge coefficient that was found in the experiment and on the discharge coefficient that was predicted using the initial model. As mentioned, the yellow cells in the table above indicate uncertainty whether there was perfect or imperfect flow. For these cases, bother perfected and imperfect flow are modelled. are predicted with the model.

Because the measurement equipment has a significance of 0.2-0.3 mm (as stated in section 3.1.2), all measurements are written with a significance in mm.

Table 6 The experiment results and corresponding model predictions. C_p denotes the discharge coefficient of a perfect weir and C_i denotes the discharge coefficient of an imperfect weir. The one that is used depends on the measurement. For each flow conditions, there are different models that are used to make predictions about the discharge coefficient.

	$Q = 29.3$ [l/s]		$h_2 \cong 0.179$ [m]						
Weir configuration	$h_2\ [m]$	$h_0[m]$	$C_{p;exp}$ OR $C_{i;exp}$	$C_{p;Reh;avg}$	$C_{p;Reh;indv}$	$C_{i;mom;avg}$	$C_{i;mom;indv}$	$C_{i;Carnot;avg}$	$C_{i;Carnot;indv}$
1	0.179	0.181	0.449			0.993	0.993	0.794	0.794
2	0.179	0.181	0.536			0.855	0.912	0.813	0.801
3	0.179	0.181	0.612			0.855	0.913	0.813	0.801
4	0.179	0.181	0.547			0.855	0.913	0.813	0.801

5	0.179	0.181	0.649			0.780	0.943	0.811	0.786
6	0.179	0.181	0.635			0.779	0.943	0.811	0.786
7	0.179	0.181	0.676			0.780	0.888	0.811	0.794
8	0.179	0.181	0.686			0.780	0.889	0.811	0.794
9	0.179	0.181	0.684			0.780	0.780	0.811	0.811
10	0.180	0.189	0.864	0.704	0.704				
11	0.178	0.182	0.677			0.747	0.906	0.794	0.779

	$Q = 29.3$ [l/s]		$h_2 \cong 0.161$ [m]						
Weir configuration	$h_2\ [m]$	$h_0[m]$	$C_{p;exp}$ OR $C_{i;exp}$	$C_{p;Reh;avg}$	$C_{p;Reh;indv}$	$C_{i;mom;avg}$	$C_{i;mom;indv}$	$C_{i;Carnot;avg}$	$C_{i;Carnot;indv}$
1	0.161	0.162	0.634			0.951	0.951	0.800	0.800
2	0.161	0.163	0.647			0.823	0.882	0.815	0.801
3	0.161	0.163	0.699			0.823	0.882	0.815	0.801
4	0.161	0.163	0.690			0.823	0.882	0.815	0.801
5	0.161	0.164	0.779			0.756	0.929	0.799	0.793
6	0.161	0.164	0.743			0.756	0.928	0.799	0.793
7	0.161	0.164	0.720			0.756	0.870	0.799	0.795
8	0.161	0.164	0.787			0.757	0.871	0.800	0.795
9	0.162	0.164	0.787			0.757	0.757	0.800	0.800
10	0.159	0.180	1.315	0.700	0.700				
11	0.161	0.166	0.588	0.716	0.745				

	$Q = 59.6$ [l/s]		$h_2 \cong 0.195$ [m]						
Weir configuration	$h_2\ [m]$	$h_0[m]$	$C_{p;exp}$ OR $C_{i;exp}$	$C_{p;Reh;avg}$	$C_{p;Reh;indv}$	$C_{i;mom;avg}$	$C_{i;mom;indv}$	$C_{i;Carnot;avg}$	$C_{i;Carnot;indv}$
1	0.195	0.196	0.983			1.025	1.025	0.788	0.788
2	0.195	0.197	0.876			0.878	0.933	0.809	0.797
3	0.194	0.197	0.858			0.878	0.933	0.809	0.797
4	0.194	0.197	0.859			0.878	0.933	0.809	0.797
5	0.194	0.198	0.412 OR 0.843	0.756	0.801	0.796	0.948	0.810	0.781
6	0.194	0.198	0.412 OR 0.830	0.756	0.801	0.796	0.948	0.810	0.781
7	0.200	0.204	0.752			0.804	0.904	0.811	0.791
8	0.200	0.203	0.848			0.804	0.904	0.811	0.791
9	0.200	0.204	0.804			0.804	0.804	0.811	0.811
10	0.200	0.213	0.807	0.716	0.716				
11	0.200	0.205	0.482	0.740	0.776				

For configuration 5 and 6 it seems likely that imperfect weir flow is the case. In other measurements, configurations 5-9 all have approximately the same discharge coefficient and in this case, the discharge coefficient for imperfect flow lies close to 7-9. Based on this, 5 and 6 are considered imperfect flow.

	$Q = 59.6$ [l/s]		$h_2 \cong 0.173$ [m]						
Weir configuration	$h_2\ [m]$	$h_0[m]$	$C_{p;exp}$ OR $C_{i;exp}$	$C_{p;Reh;avg}$	$C_{p;Reh;indv}$	$C_{i;mom;avg}$	$C_{i;mom;indv}$	$C_{i;Carnot;avg}$	$C_{i;Carnot;indv}$
1	0.174	0.175	1.210			0.976	0.976	0.794	0.794
2	0.174	0.176	1.032			0.841	0.896	0.811	0.797
3	0.174	0.176	0.390 OR 1.083	0.782	0.801	0.841	0.897	0.811	0.797
4	0.173	0.176	0.390 OR 1.067	0.782	0.801	0.841	0.897	0.811	0.797
5	0.173	0.179	0.576	0.742	0.782				
6	0.172	0.179	0.576	0.742	0.782				
7	0.173	0.179	0.574	0.742	0.769				
8	0.173	0.179	0.573	0.742	0.769				
9	0.174	0.180	0.565	0.743	0.743				
10	0.174	0.201	1.124	0.710	0.710				
11	0.172	0.182	0.760	0.726	0.758				

Configurations 3 and 4 seem to have discharge coefficients that are too high. Seems to be the same for configuration 2, which has the same average height. Even though the coefficient is clearly wrong, 3 and 4 can be considered imperfect because they are so closely related to configuration 2.

	$Q = 34.0$ [l/s]		$h_2 \cong 0.180$ [m]						
Weir configuration	$h_2\ [m]$	$h_0[m]$	$C_{p;exp}$ OR $C_{i;exp}$	$C_{p;Reh;avg}$	$C_{p;Reh;indv}$	$C_{i;mom;avg}$	$C_{i;mom;indv}$	$C_{i;Carnot;avg}$	$C_{i;Carnot;indv}$
5	0.180	0.183	0.645			0.781	0.943	0.810	0.785
6	0.180	0.183	0.612			0.780	0.942	0.810	0.785
7	0.180	0.183	0.627			0.781	0.888	0.810	0.794

	$Q = 34.0$ [l/s]		$h_2 \cong 0.156$ [m]						
Weir configuration	$h_2\ [m]$	$h_0[m]$	$C_{p;exp}$ OR $C_{i;exp}$	$C_{p;Reh;avg}$	$C_{p;Reh;indv}$	$C_{i;mom;avg}$	$C_{i;mom;indv}$	$C_{i;Carnot;avg}$	$C_{i;Carnot;indv}$
5	0.156	0.161	0.725			0.749	0.922	0.791	0.756
6	0.157	0.161	0.735			0.750	0.922	0.791	0.796
7	0.156	0.161	0.726			0.749	0.864	0.791	0.766

	$Q = 73.8$ [l/s]		$h_2 \cong 0.176$ [m]						
Weir configuration	$h_2\ [m]$	$h_0[m]$	$C_{p;exp}$ OR $C_{i;exp}$	$C_{p;Reh;avg}$	$C_{p;Reh;indv}$	$C_{i;mom;avg}$	$C_{i;mom;indv}$	$C_{i;Carnot;avg}$	$C_{i;Carnot;indv}$
5	0.176	0.184	0.639	0.746	0.788				
6	0.176	0.184	0.636	0.746	0.788				
7	0.176	0.185	0.633	0.746	0.774				

D.2 Bar plots of model and measurements

The measurements are plotted in the following bar plots:

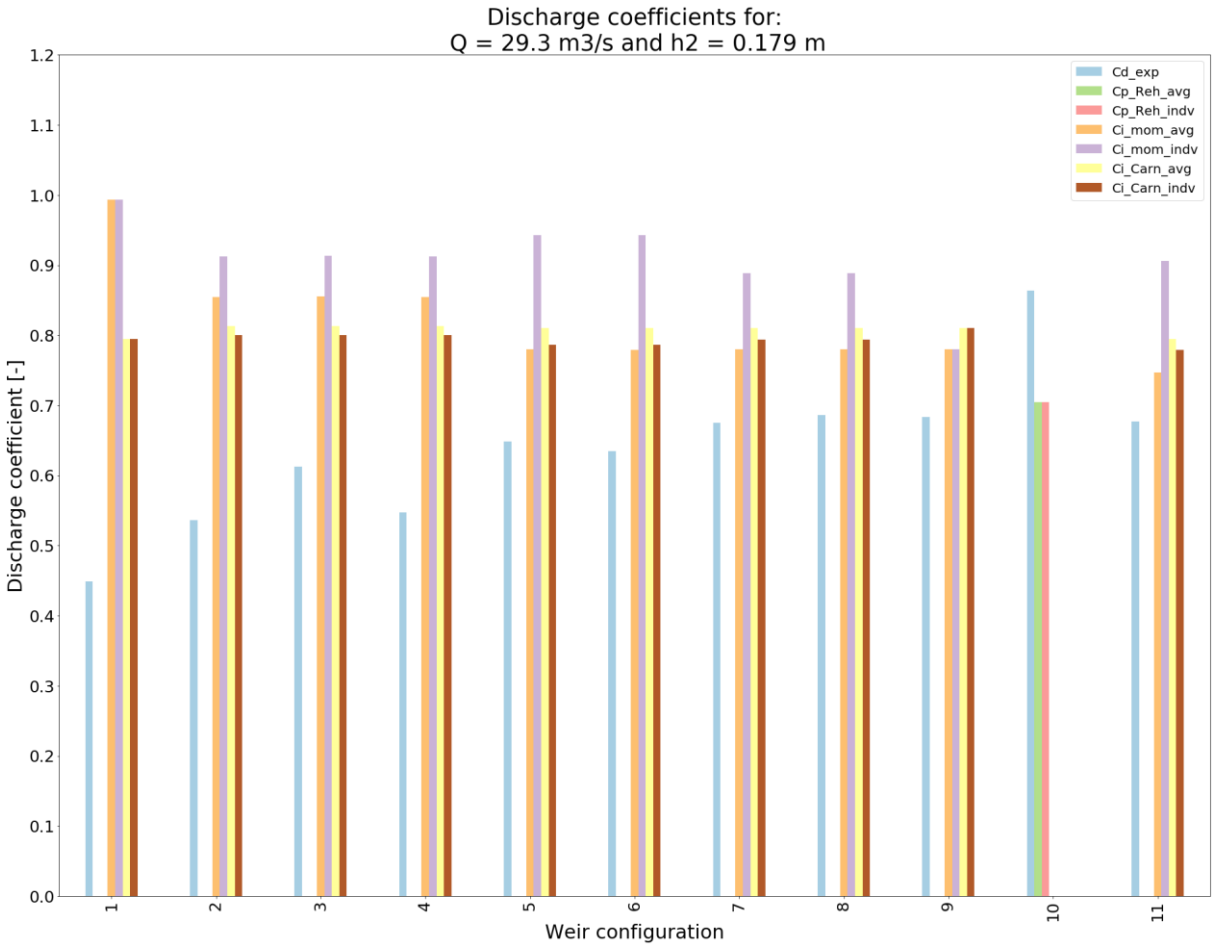

Figure 21 Discharge coefficients for different configurations. The flow conditions are indicated at the top of the plot. Whether the discharge coefficient is calculated for perfect or imperfect flow is indicated by which predictions are made. Rehbock indicates perfect flow and momentum and Carnot indicate imperfect flow.

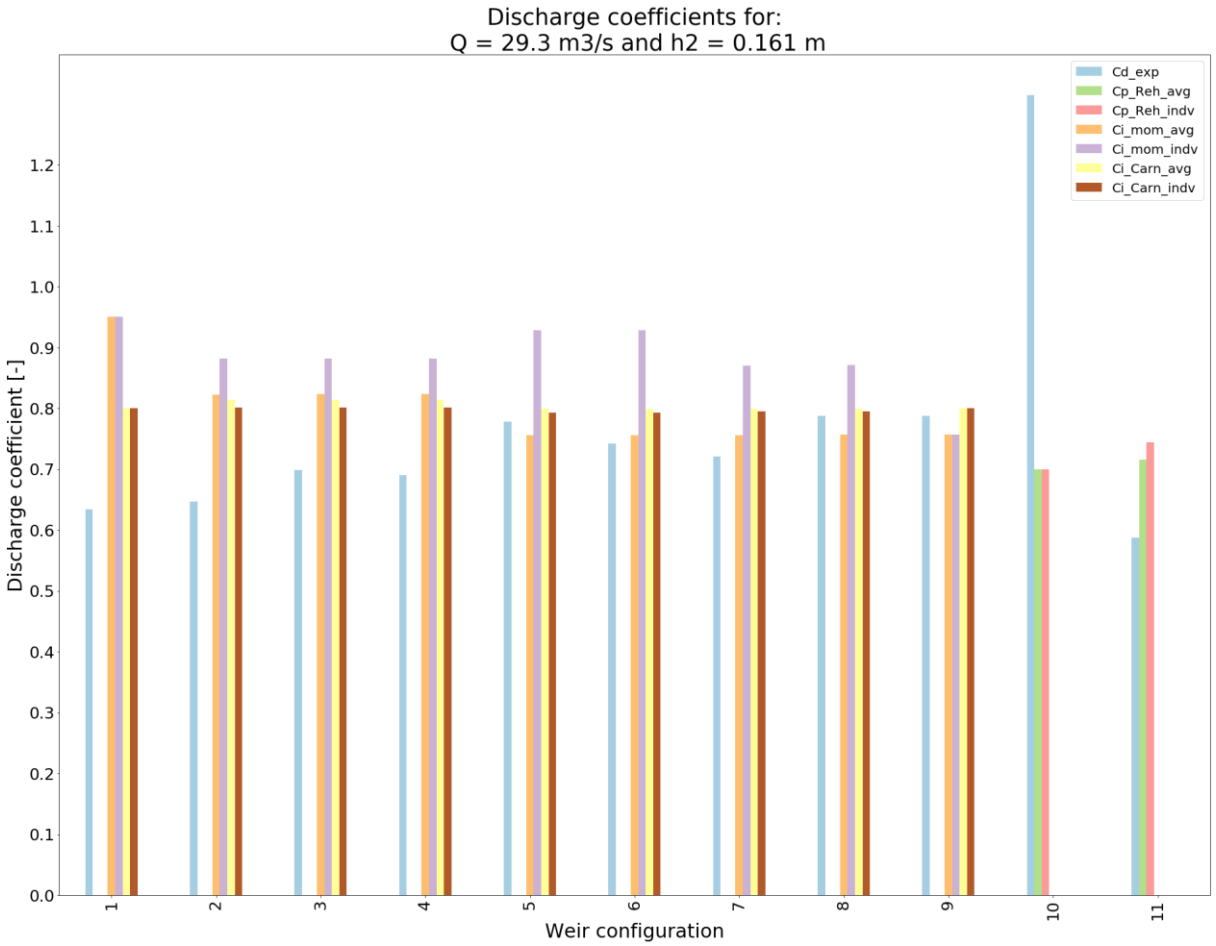

Figure 22 Discharge coefficients for different configurations. The flow conditions are indicated at the top of the plot. Whether the discharge coefficient is calculated for perfect or imperfect flow is indicated by which predictions are made. Rehbock indicates perfect flow and momentum and Carnot indicate imperfect flow.

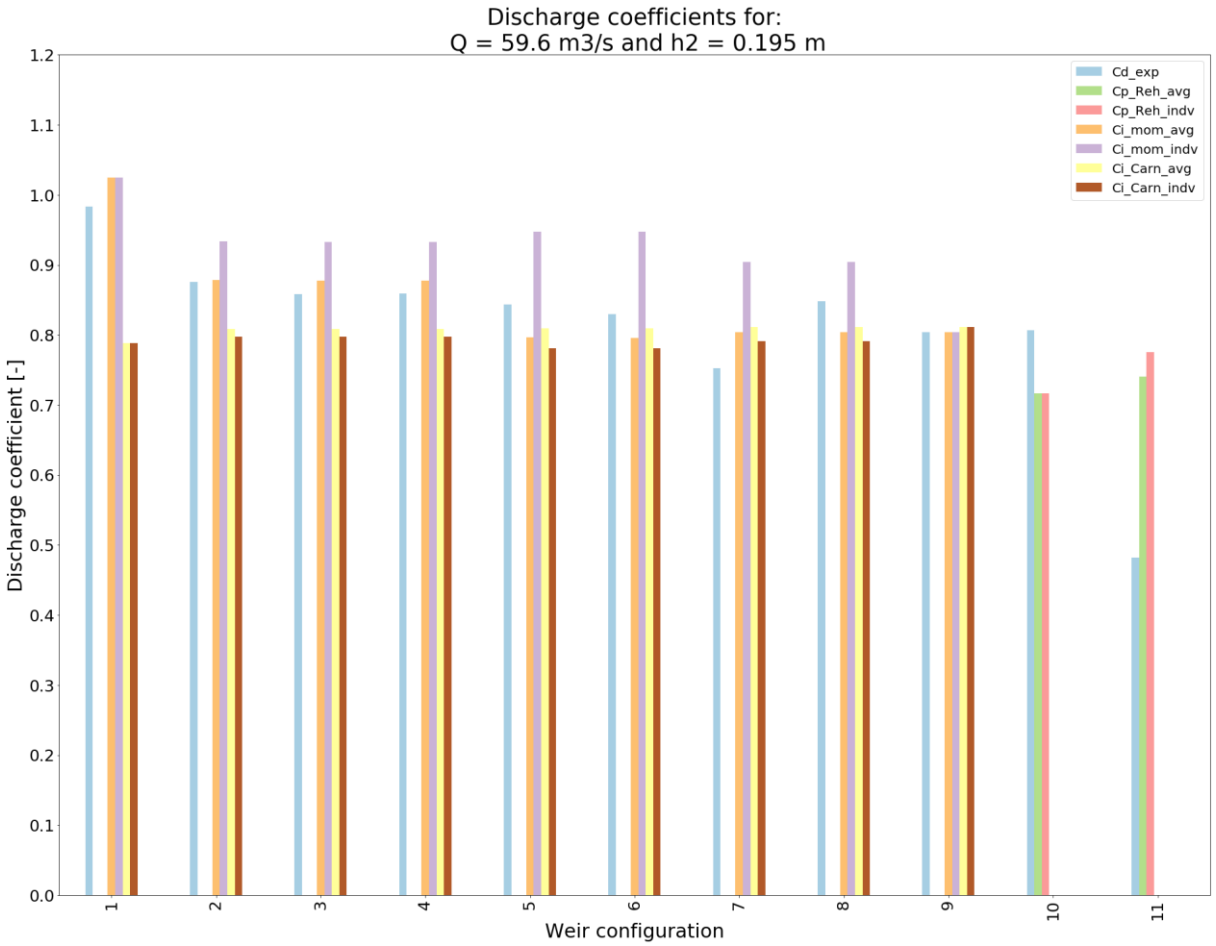

Figure 23 Discharge coefficients for different configurations. The flow conditions are indicated at the top of the plot. Whether the discharge coefficient is calculated for perfect or imperfect flow is indicated by which predictions are made. Rehbock indicates perfect flow and momentum and Carnot indicate imperfect flow.

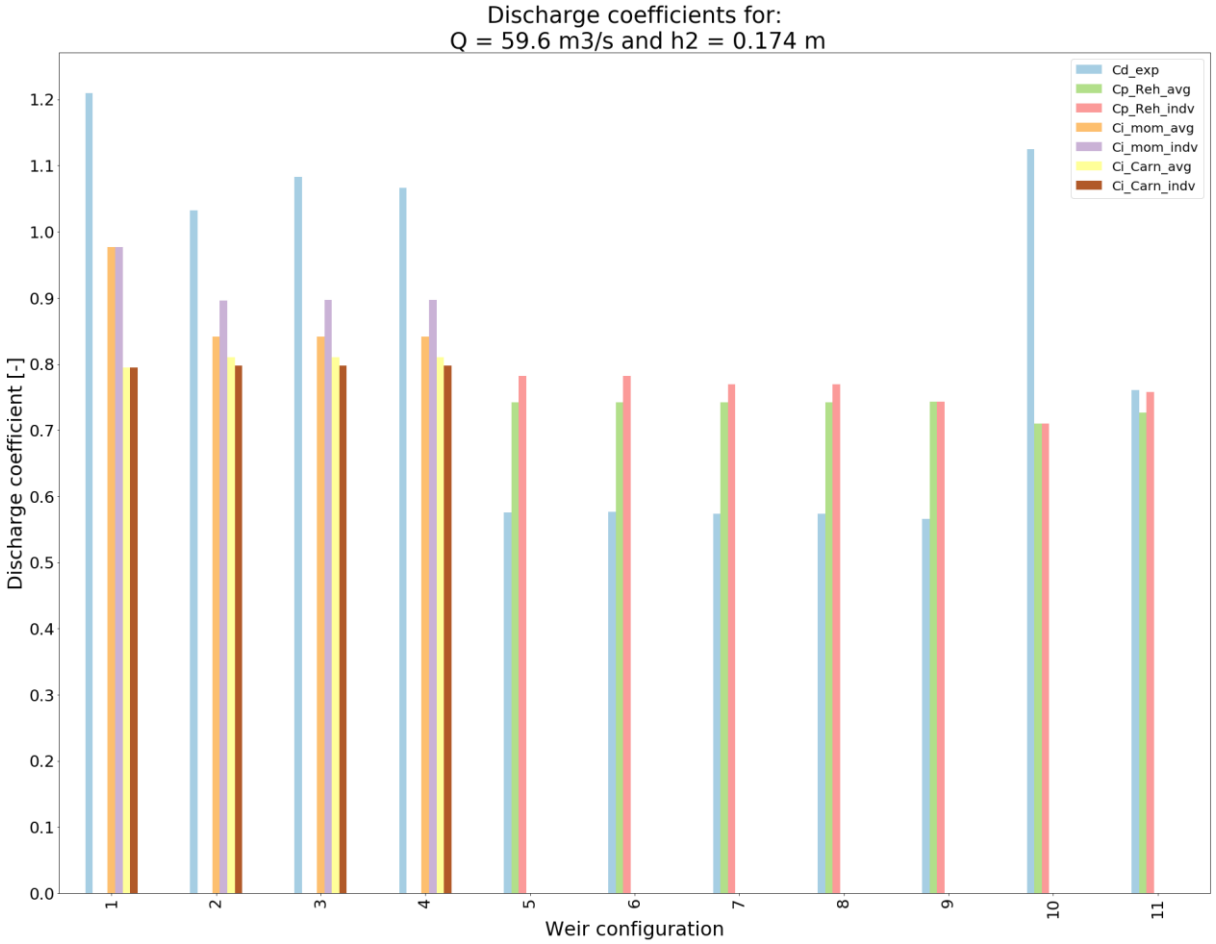

Figure 24 Discharge coefficients for different configurations. The flow conditions are indicated at the top of the plot. Whether the discharge coefficient is calculated for perfect or imperfect flow is indicated by which predictions are made. Rehbock indicates perfect flow and momentum and Carnot indicate imperfect flow.

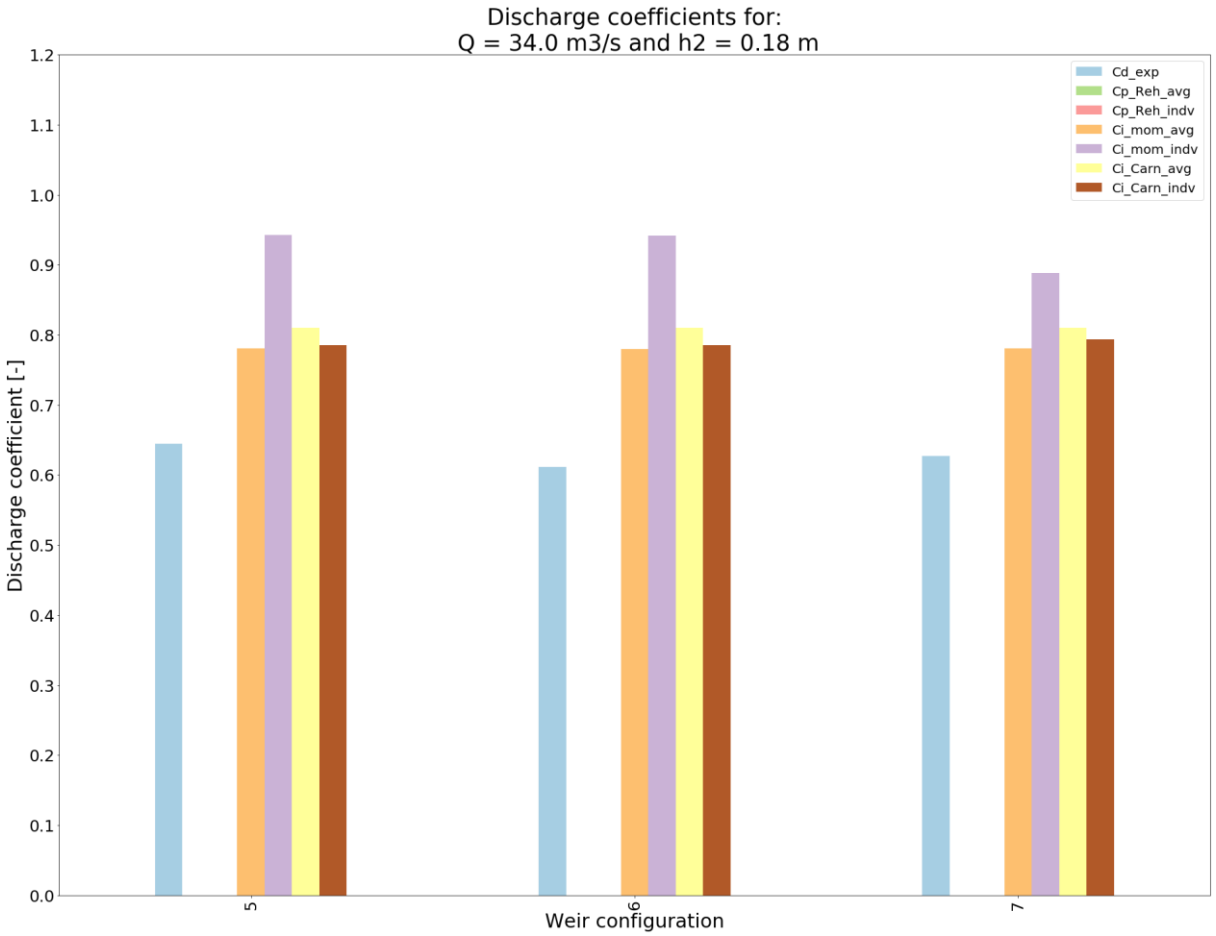

Figure 25 Discharge coefficients for different configurations. The flow conditions are indicated at the top of the plot. Whether the discharge coefficient is calculated for perfect or imperfect flow is indicated by which predictions are made. Rehbock indicates perfect flow and momentum and Carnot indicate imperfect flow. This flow condition only contains three configurations because this data was collected alongside videos to be used for PIV. Only three configurations were selected for PIV.

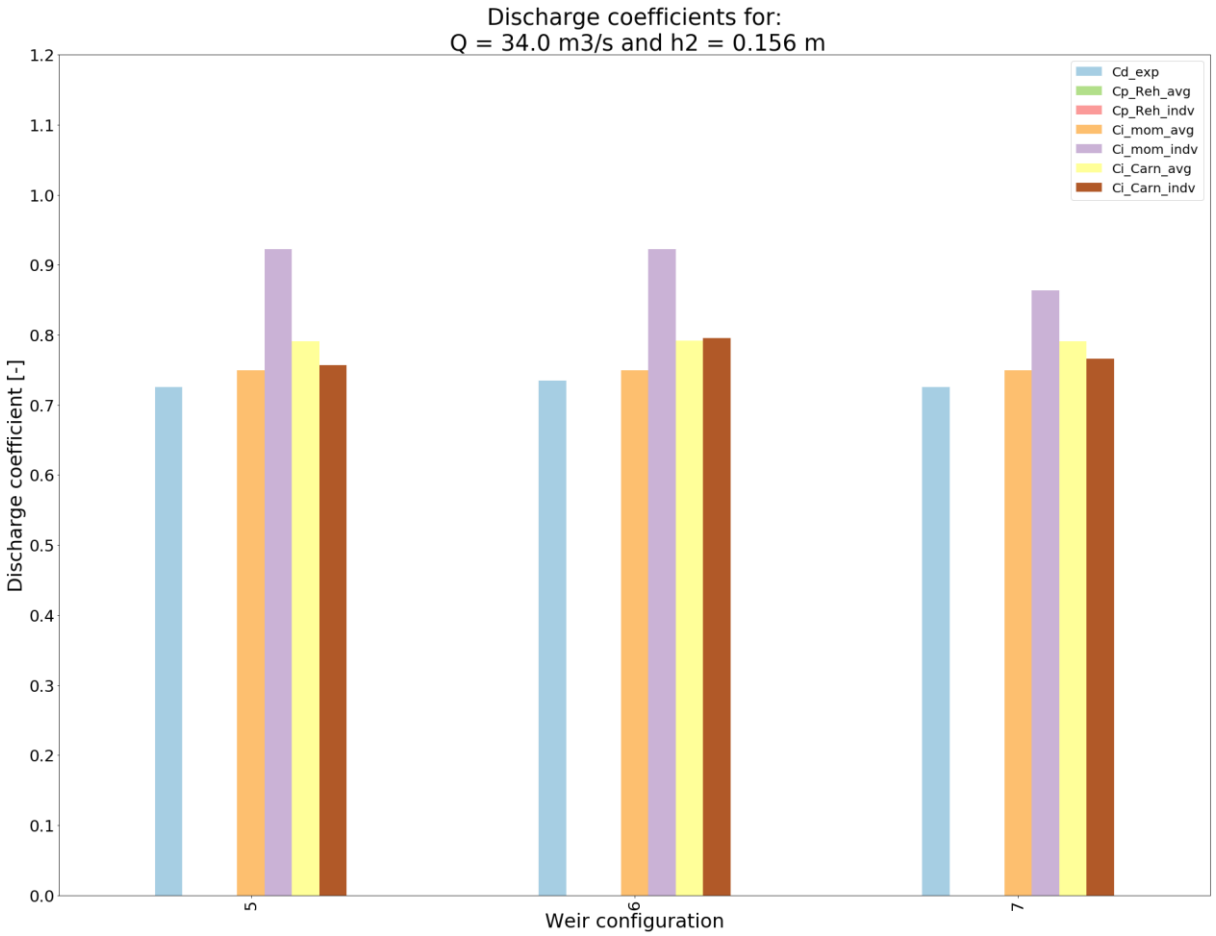

Figure 26 Discharge coefficients for different configurations. The flow conditions are indicated at the top of the plot. Whether the discharge coefficient is calculated for perfect or imperfect flow is indicated by which predictions are made. Rehbock indicates perfect flow and momentum and Carnot indicate imperfect flow. This flow condition only contains three configurations because this data was collected alongside videos to be used for PIV. Only three configurations were selected for PIV.

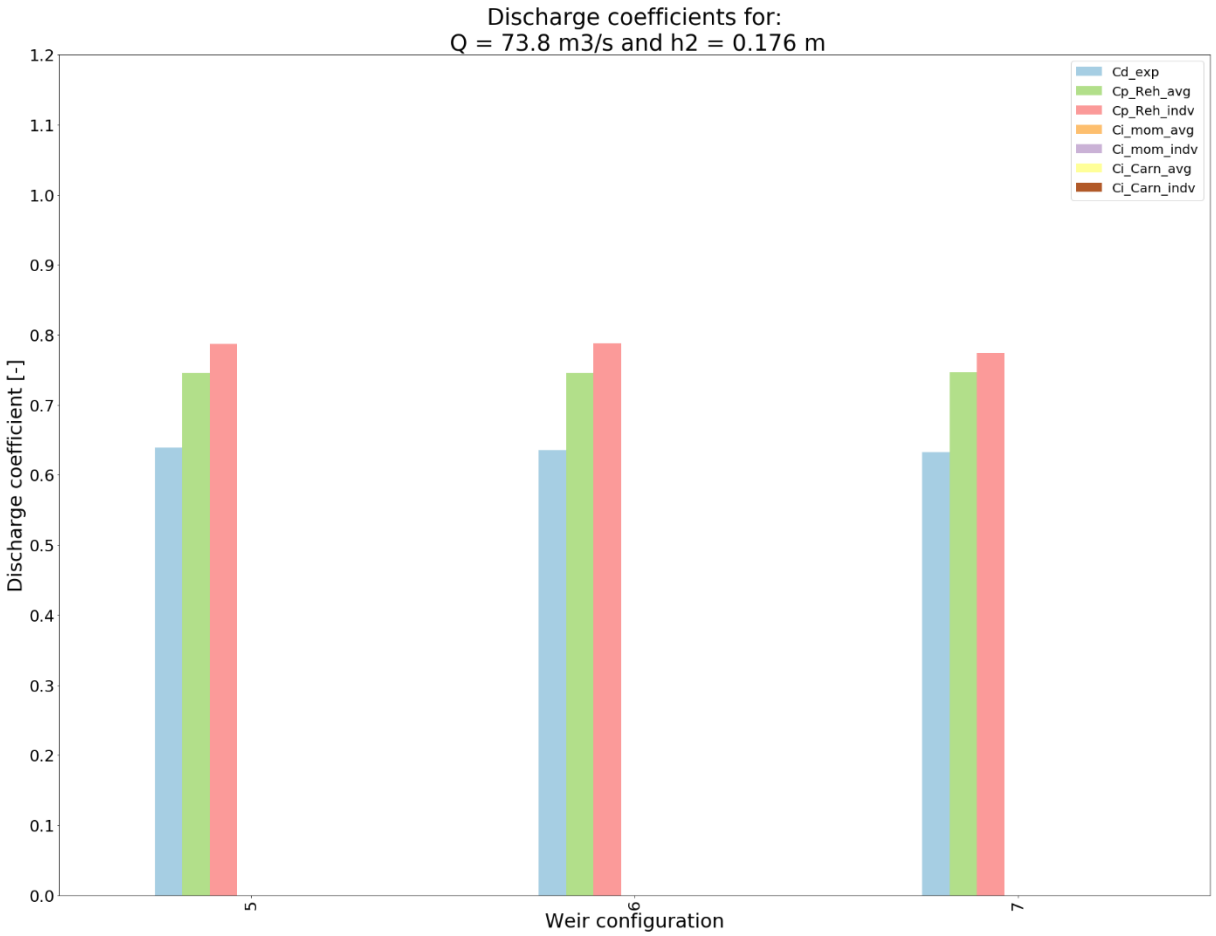

Figure 27 Discharge coefficients for different configurations. The flow conditions are indicated at the top of the plot. Whether the discharge coefficient is calculated for perfect or imperfect flow is indicated by which predictions are made. Rehbock indicates perfect flow and momentum and Carnot indicate imperfect flow. This flow condition only contains three configurations because this data was collected alongside videos to be used for PIV. Only three configurations were selected for PIV.

D.3 Scatter plots of model and measurements

In the following plots, the discharge coefficients that were calculated with the model are plotted against the measured discharge coefficient. A line is plotted in the middle. This is the scenario in which both the modelled and experimental coefficients are equal. The first set of plots contains the coefficients in the case of imperfect weir conditions.

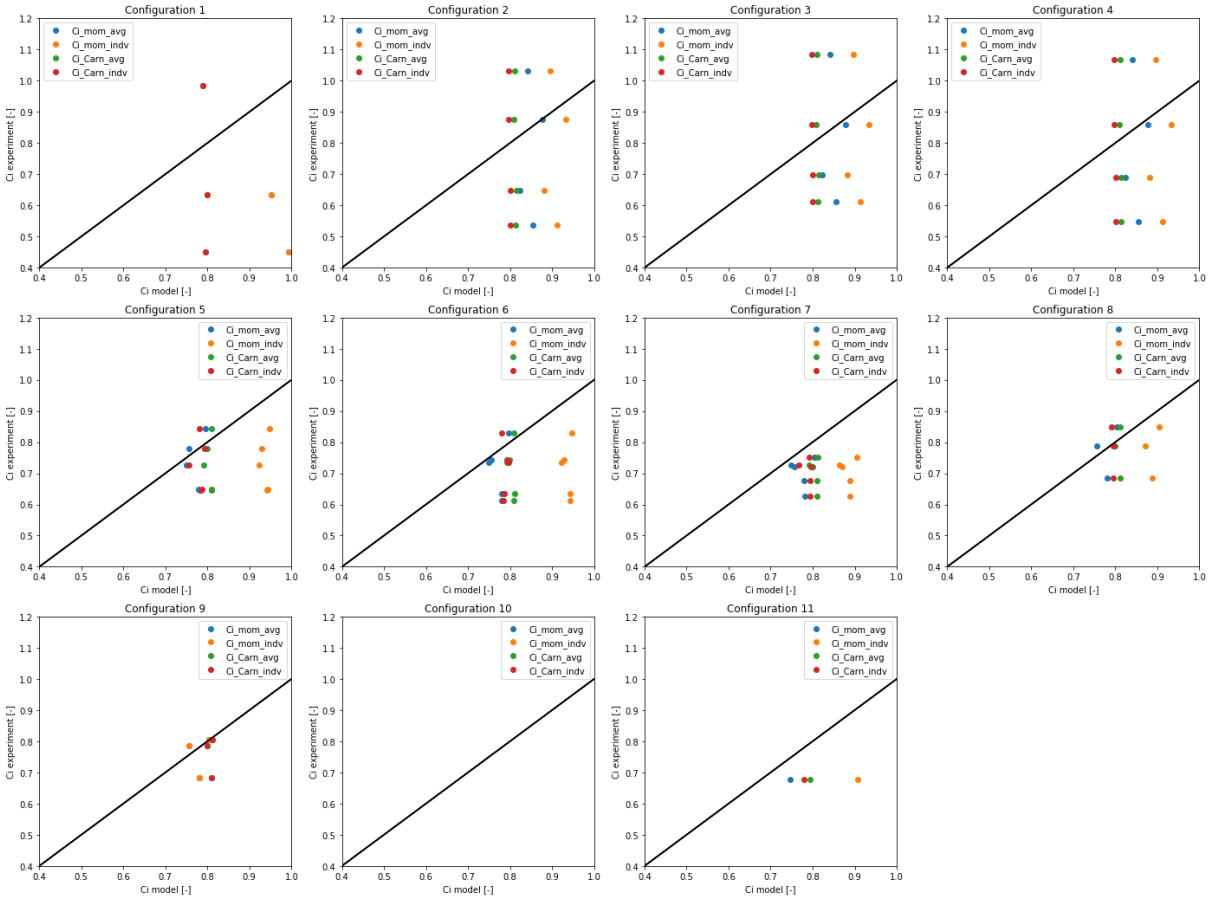

Figure 28 Scatterplots with the modelled discharge coefficients on the x-axis and the experimental discharge coefficient on the y-axis. The black line indicates y = x, which would be the ideal case. The above plots are for imperfect flow. The amount of points that are plotted depends on how much data was collected for this configuration. No points indicate that the flow was perfect for each combination of discharge and downstream water level.

The second set of plots contains the coefficients in the case of perfect weir conditions.

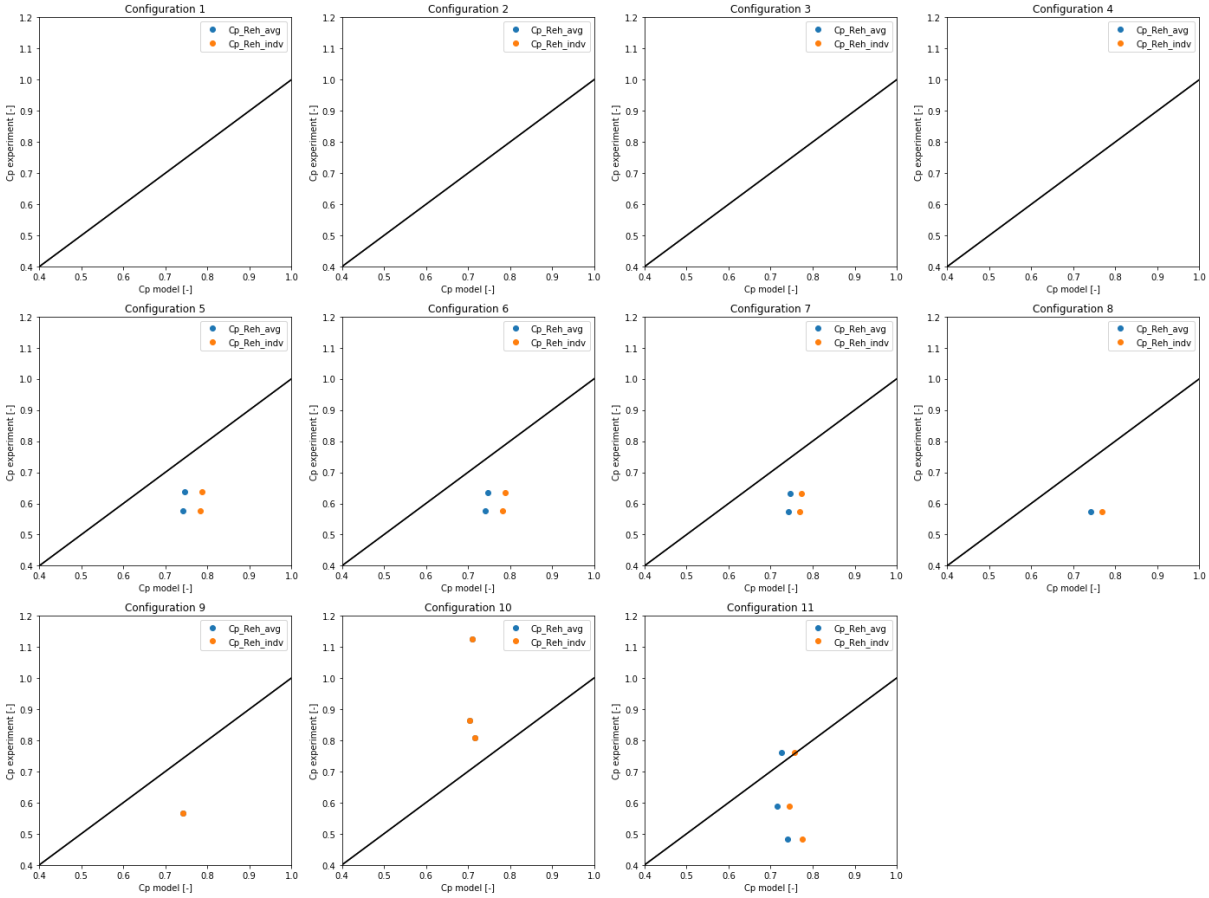

Figure 29 Scatterplots with the modelled discharge coefficients on the x-axis and the experimental discharge coefficient on the y-axis. The black line indicates y = x, which would be the ideal case. The above plots are for perfect flow. The amount of points that are plotted depends on how much data was collected for this configuration. No points indicate that the flow was imperfect for each combination of discharge and downstream water level.

D.4 PIV settings and procedure

For PIV, MATLAB was used in combination with the PIVlab app, created by William Thielicke. This is an application that lets the user input images or a video and perform PIV with settings and filters that can be configured by the user. The following settings were used:

- 12 fps: the camera shot videos with a framerate of 24 fps. It was found that the combination of size and movement speed of the particles allowed for 12 fps. This shortened the time that it took to perform PIV.
- The PIV was performed using around 60 frames, because it was found that 5s is the timescale over which a particle passed over the compound weir.
- The contrast of the image was enhanced using the recommended settings of Contrast Limited Adaptive Histogram Equalization.
- PIV was executed using the FFT window deformation algorithm.
- The algorithm starts with a grid of squares of 256 pixels and works its way down to squares of 64 pixels.
- Post processing was done based on the plausibility of velocity vectors.

For each video, the objective of the PIV is getting an image of the streamlines and a grid of velocity vectors.

D.5 PIV results

The streamlines were found by averaging the pixel values of the image.

The following section contains for configuration 5-7 images of respectively:

- Streamlines found by average pixel values
- Velocity vectors
- Velocity vectors including streamlines that were computer by following the calculated vectors.
- Velocity vectors including an indication of the velocity magnitudes. The velocity magnitude indication is qualitative.
- Velocity vectors including an indication of the velocity magnitudes and streamlines that were computer by following the calculated vectors. The velocity magnitude indication is qualitative.
- Velocity vectors including a qualitative indication of the magnitude of the lateral velocity.

Configuration 5

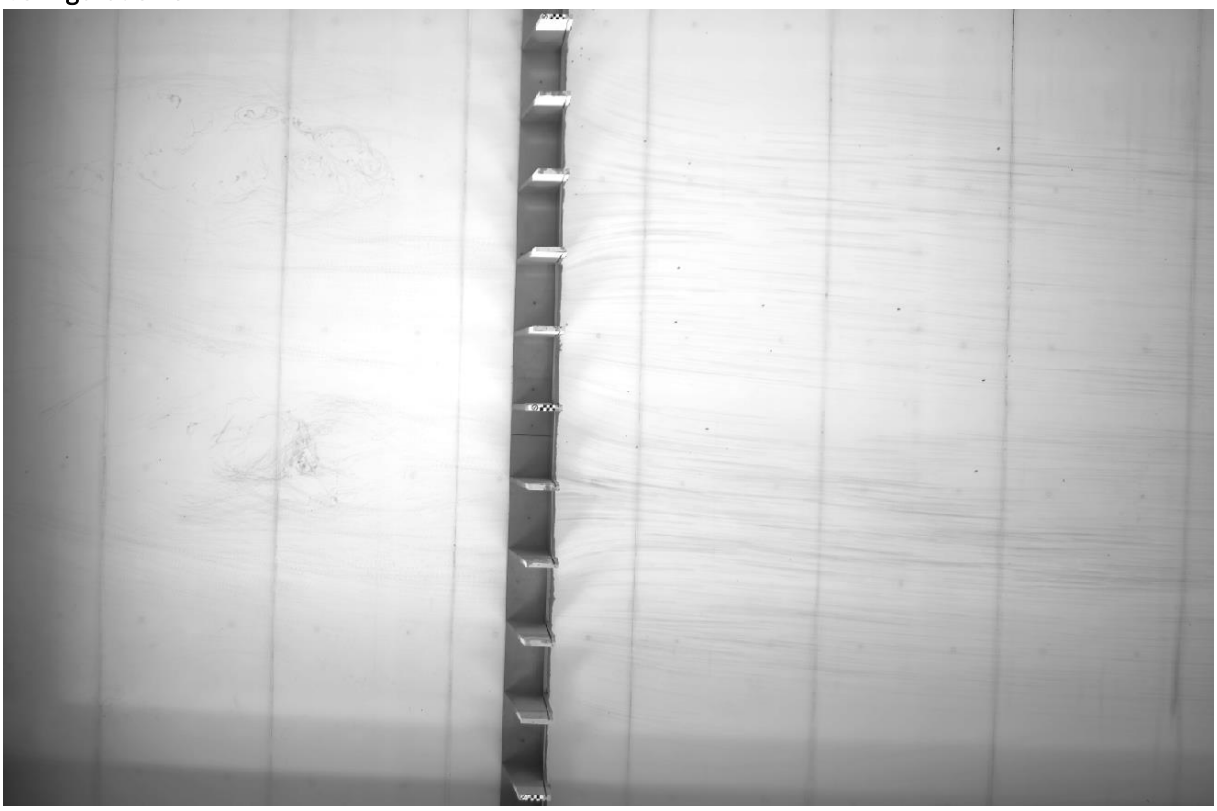

Figure 30 Streamlines of flow over configuration 5 found by average pixel values.

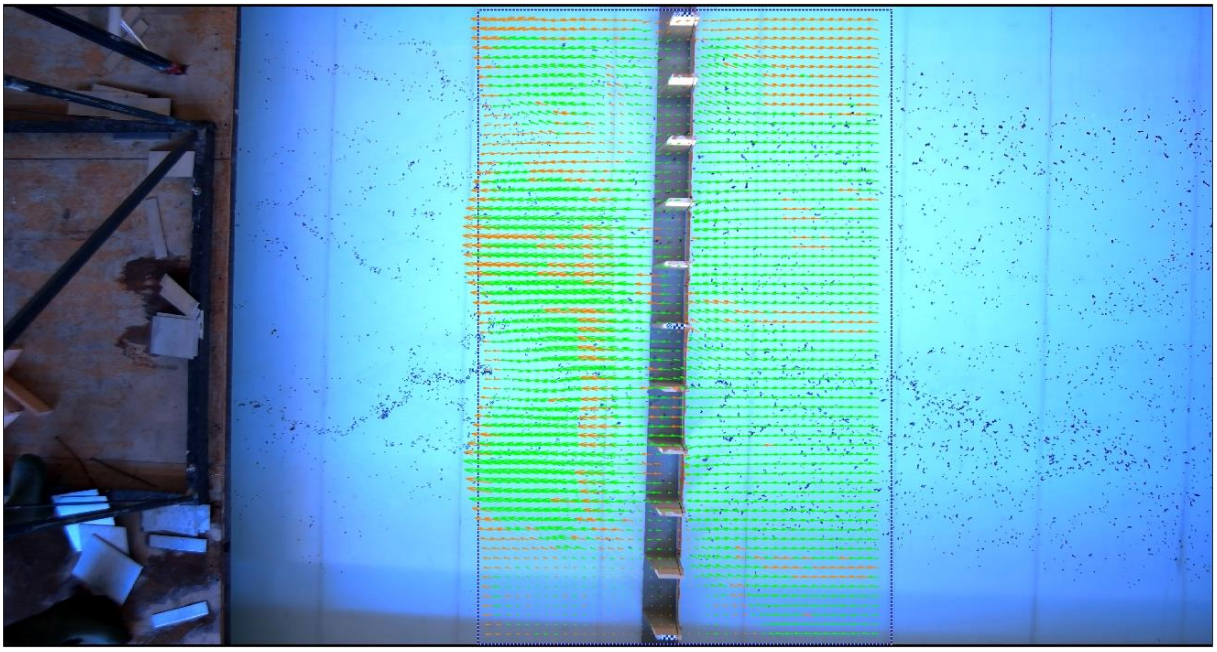

Figure 31 Velocity vectors that were found using PIV on configuration 5.

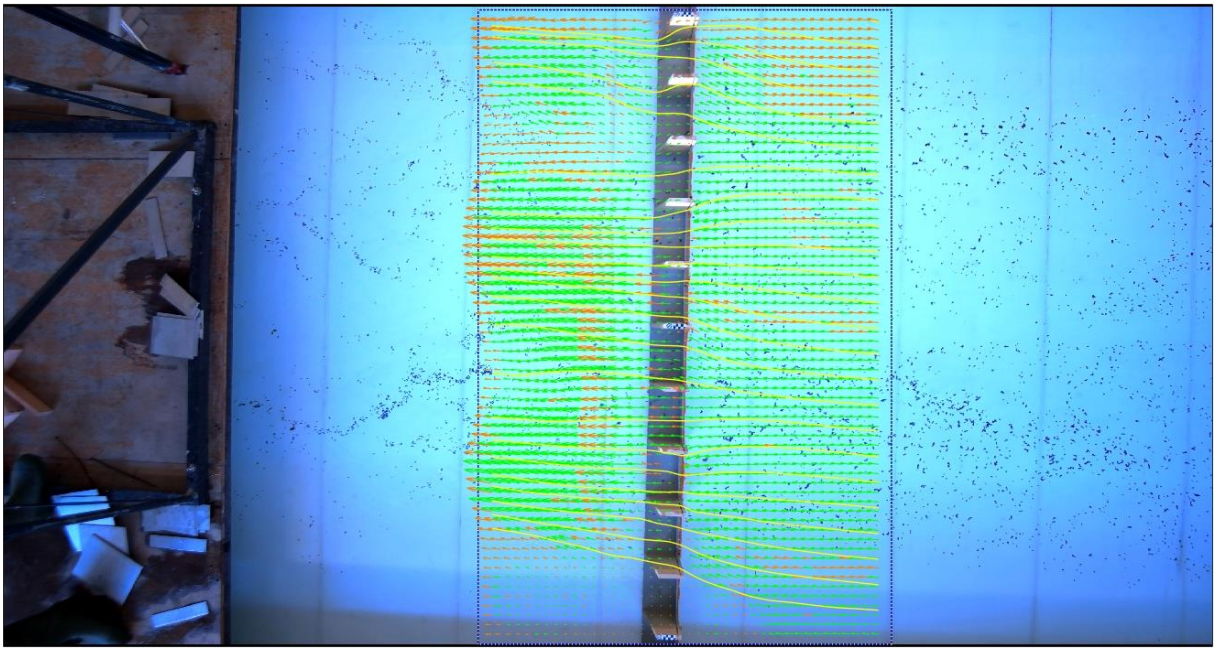

Figure 32 Velocity vectors including streamlines that were found using PIV on configuration 5.

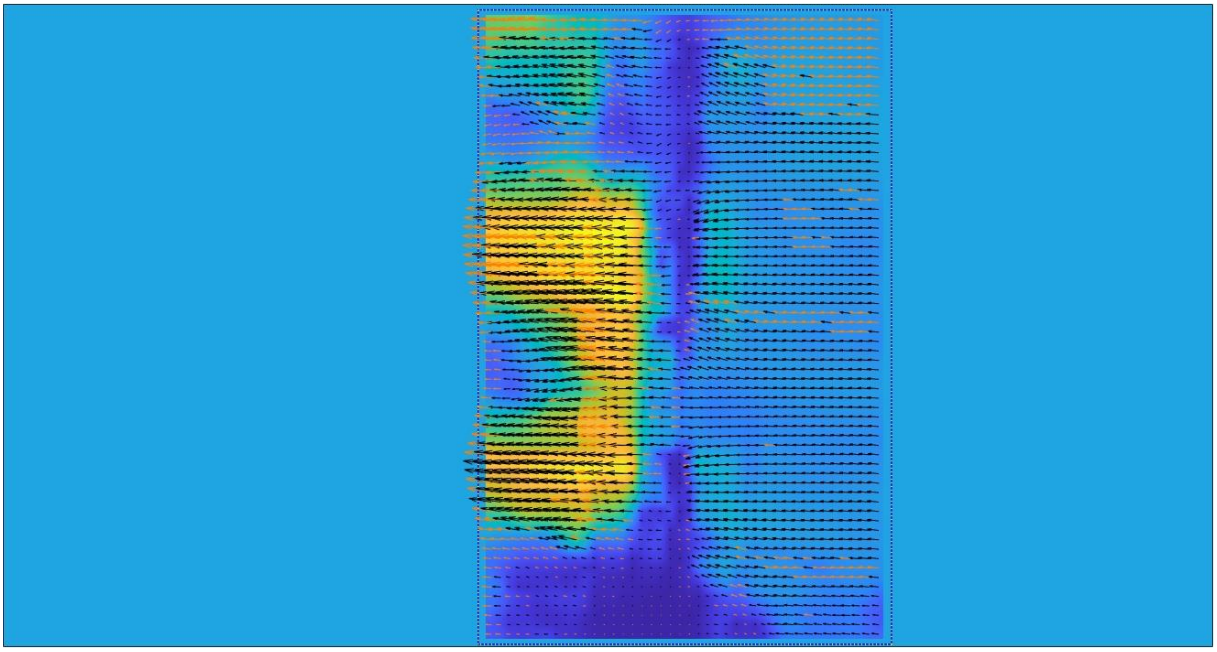

Figure 33 Qualitative velocity magnitude of configuration 5.

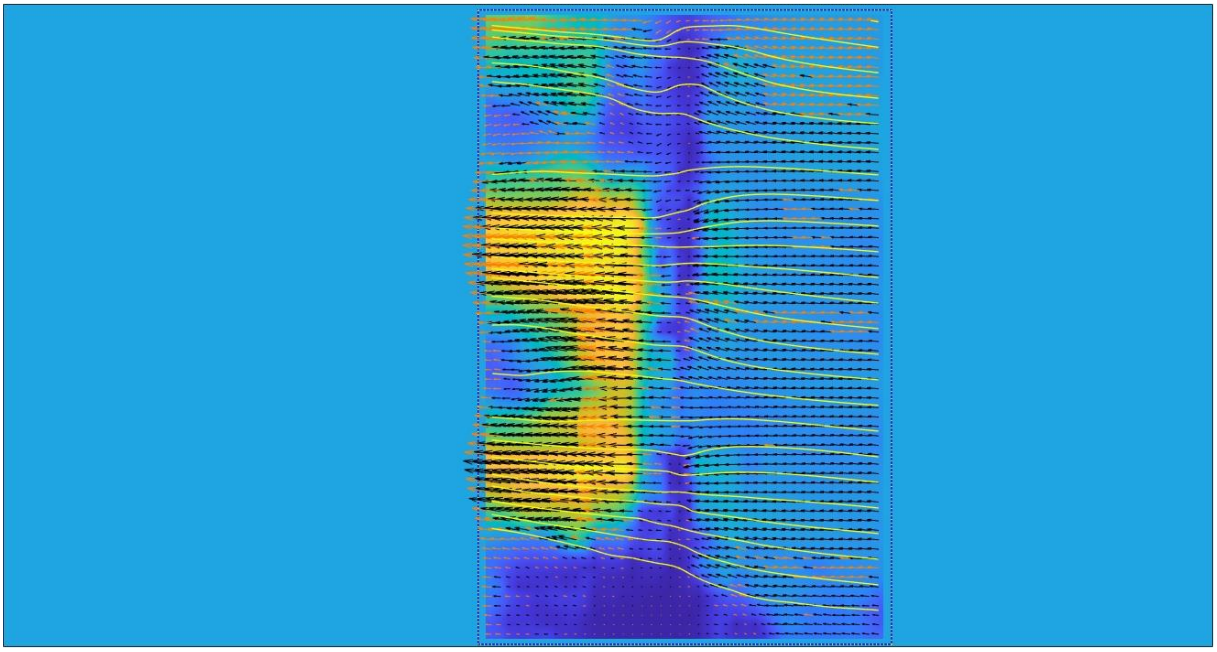

Figure 34 Qualitative velocity magnitude including streamlines of configuration 5.

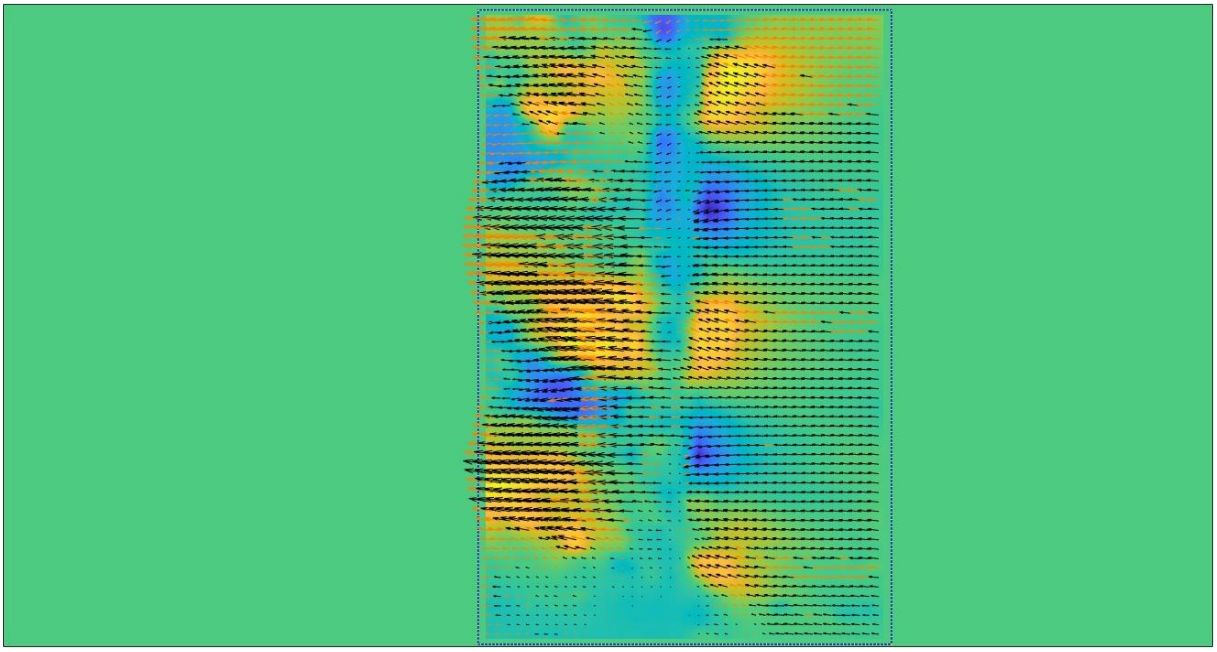

Figure 35 Qualitative magnitude of the lateral flow before and after the weir for configuration 5.

Configuration 6

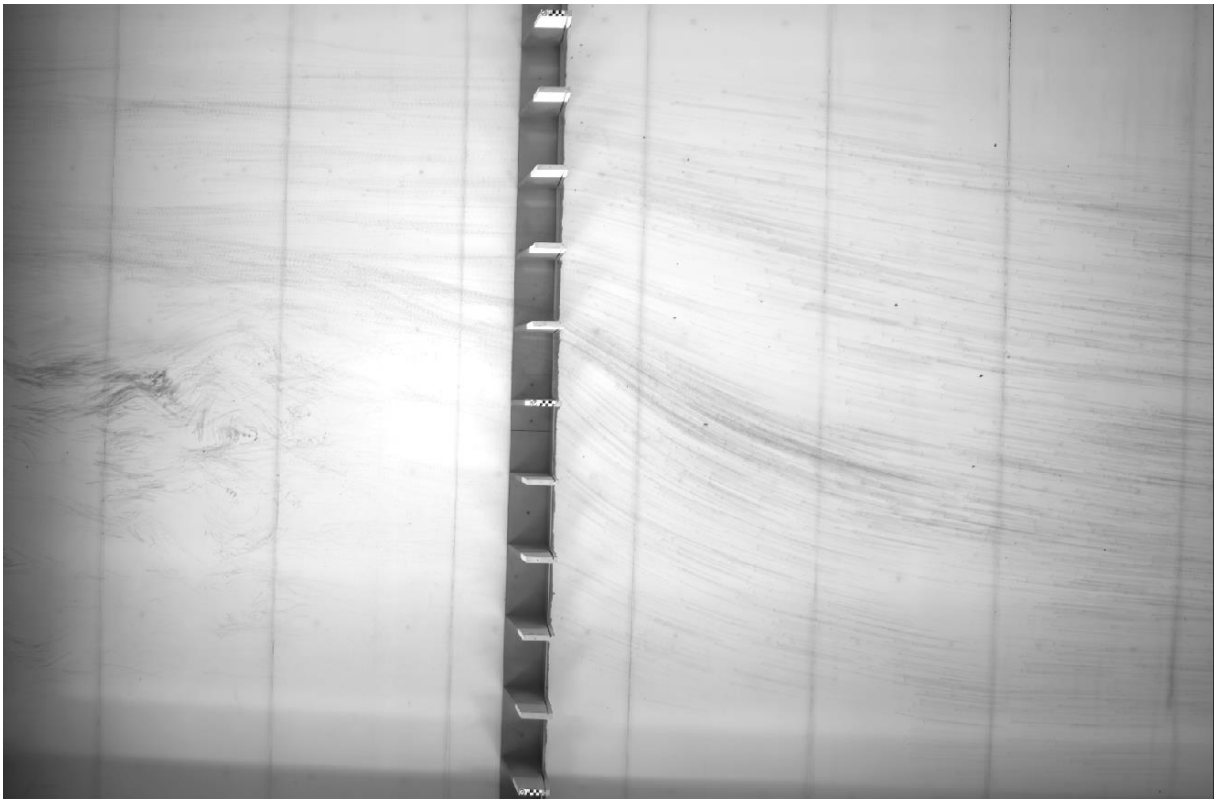

Figure 36 Streamlines of flow over configuration 6 found by average pixel values.

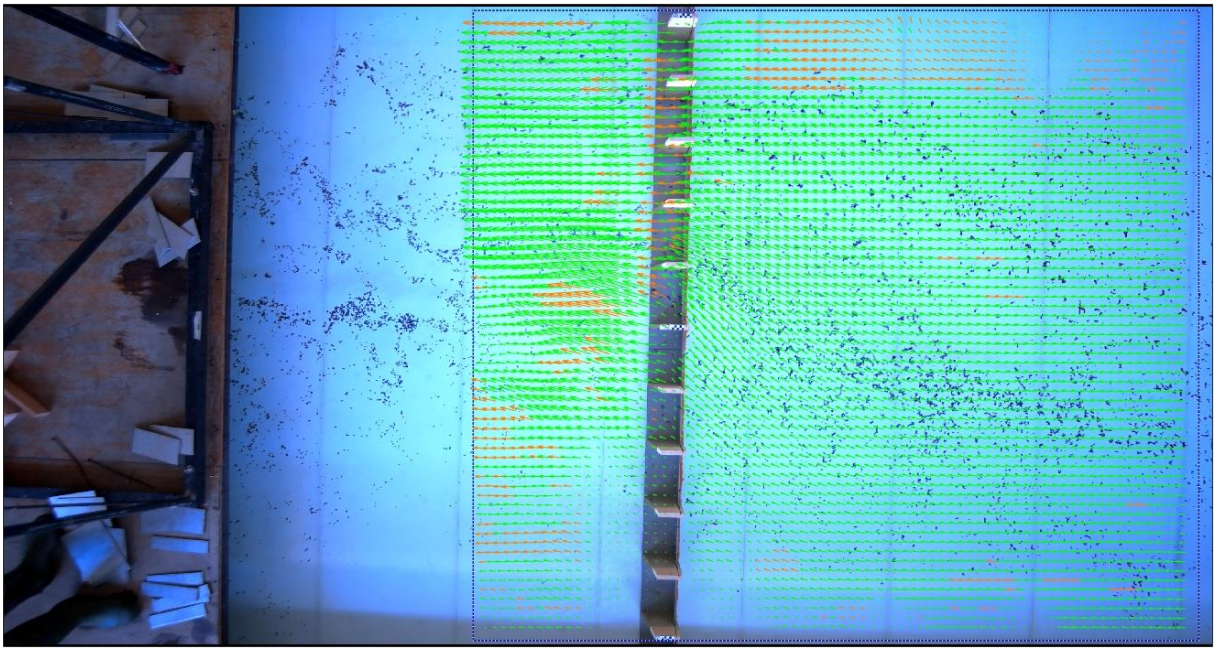

Figure 37 Velocity vectors that were found using PIV on configuration 6.

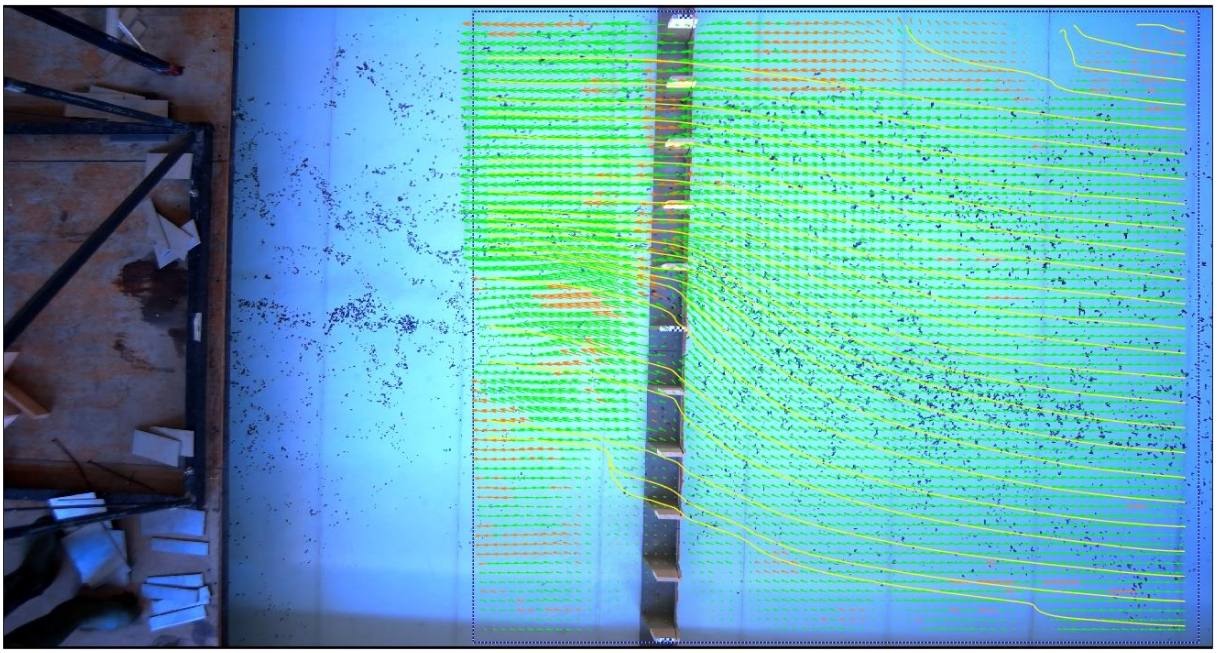

Figure 38 Velocity vectors including streamlines that were found using PIV on configuration 6.

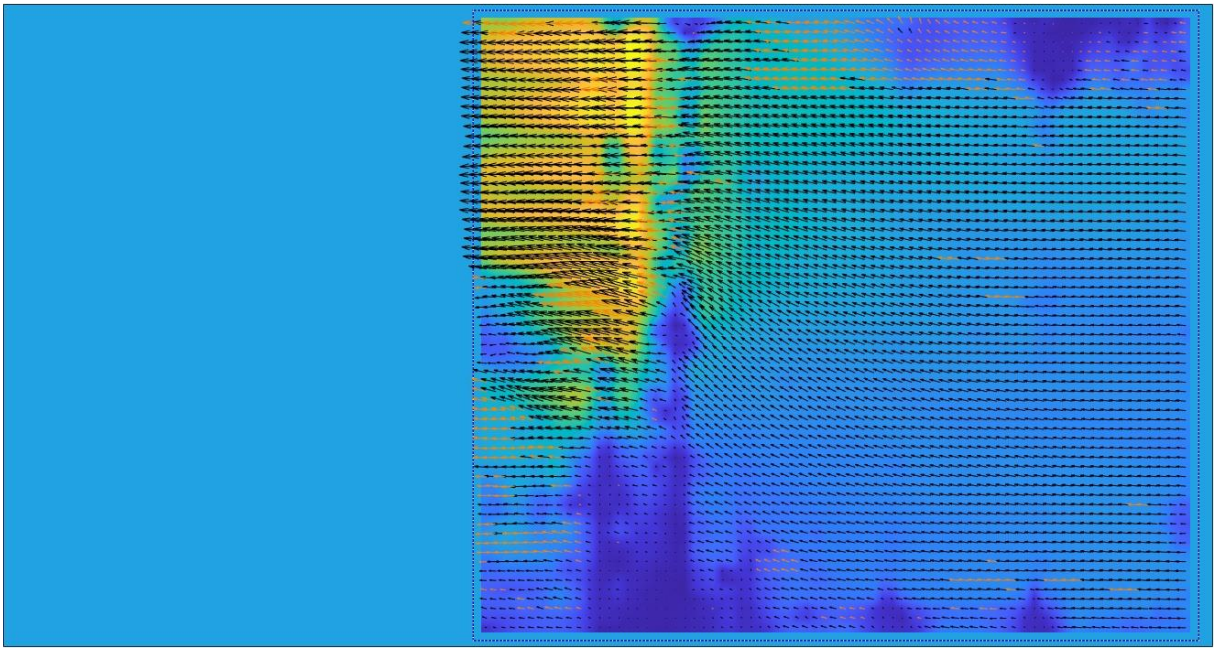

Figure 39 Qualitative velocity magnitude of configuration 6.

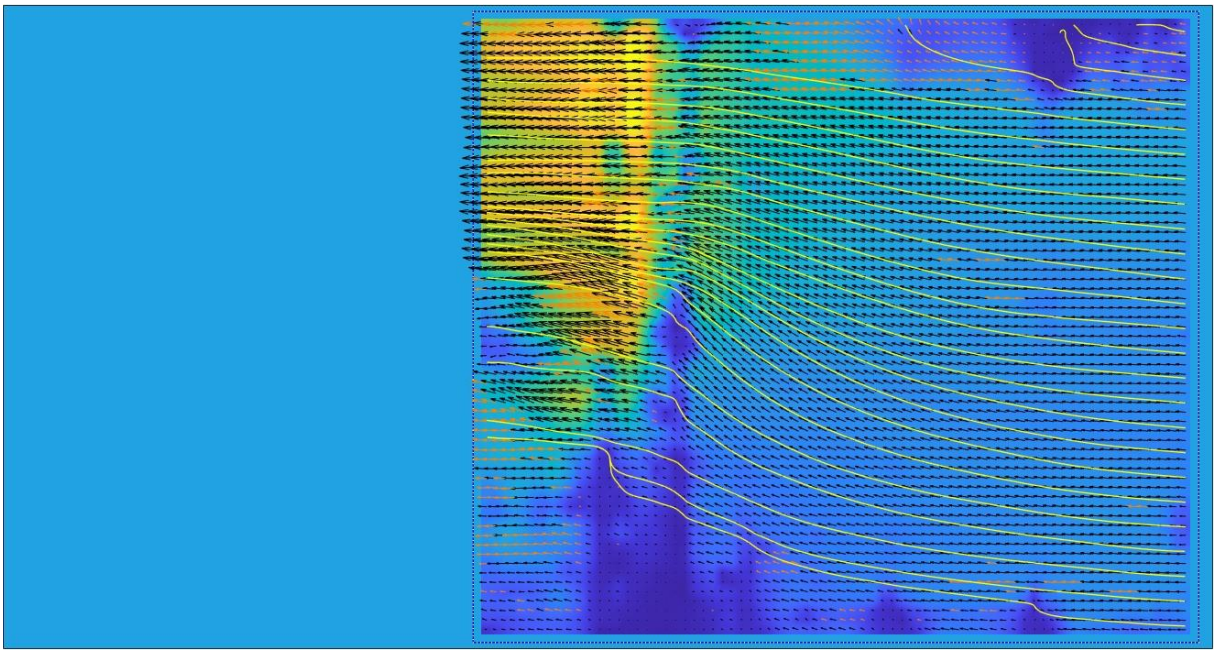

Figure 40 Qualitative velocity magnitude including streamlines of configuration 6.

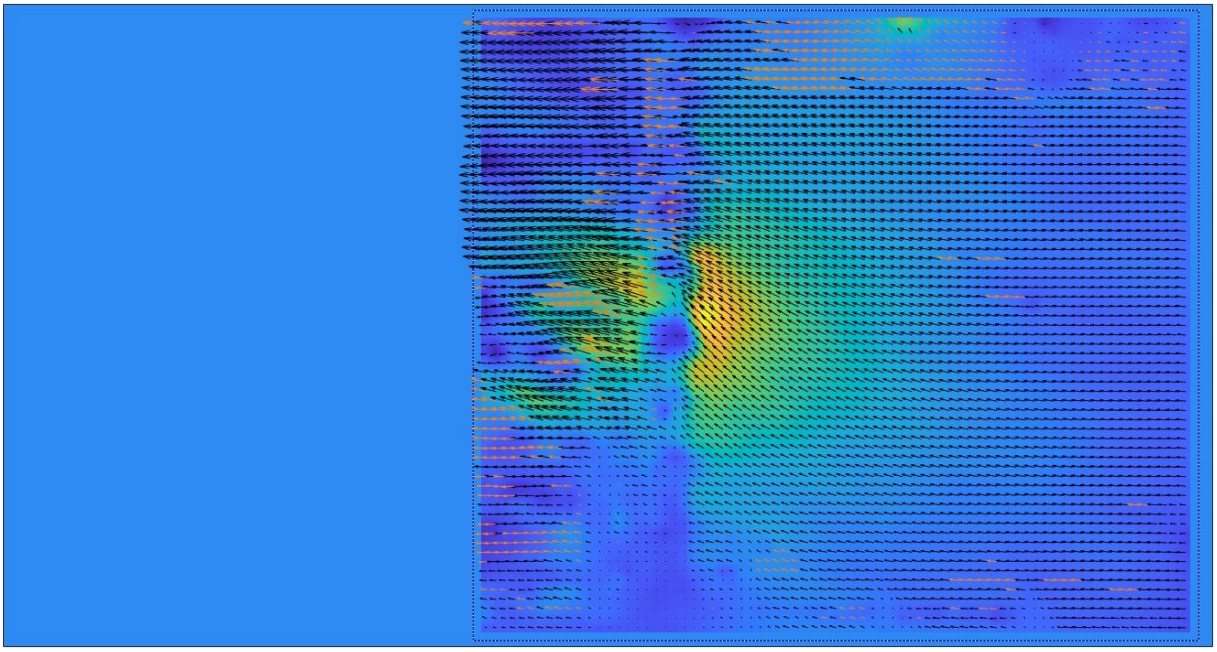

Figure 41 Qualitative magnitude of the lateral flow before and after the weir for configuration 6.

Configuration 7

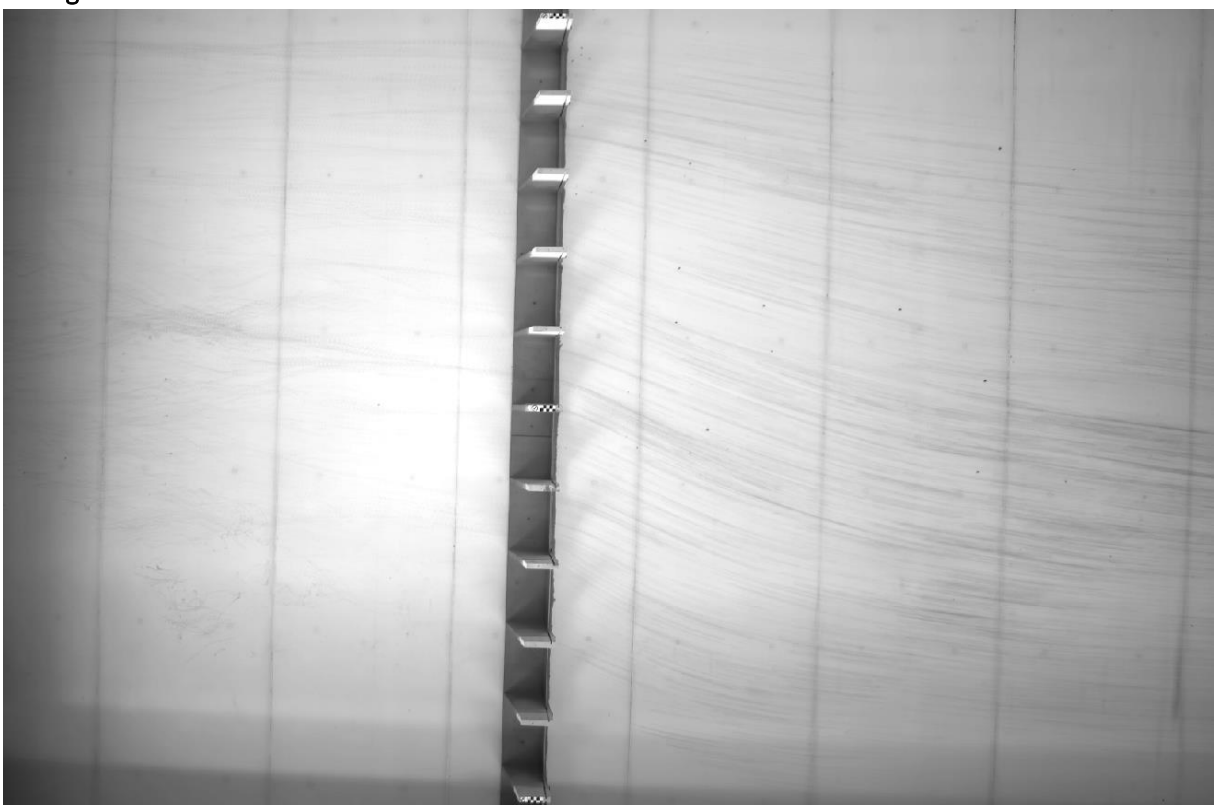

Figure 42 Streamlines of flow over configuration 7 found by average pixel values.

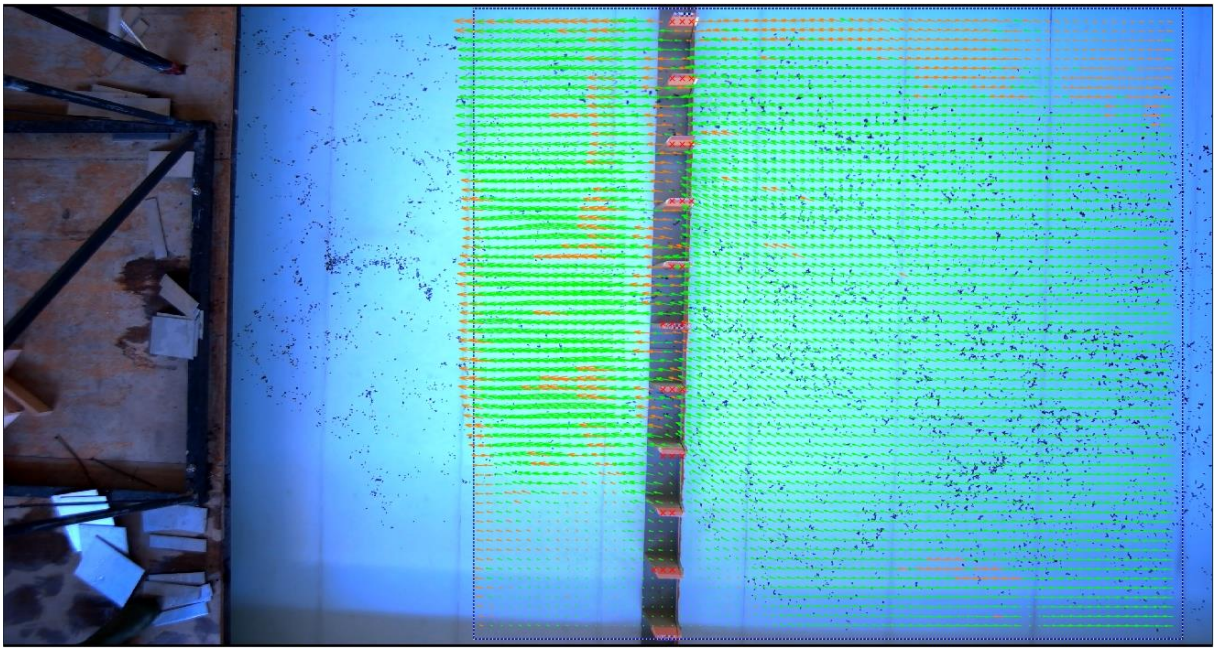

Figure 43 Velocity vectors that were found using PIV on configuration 7.

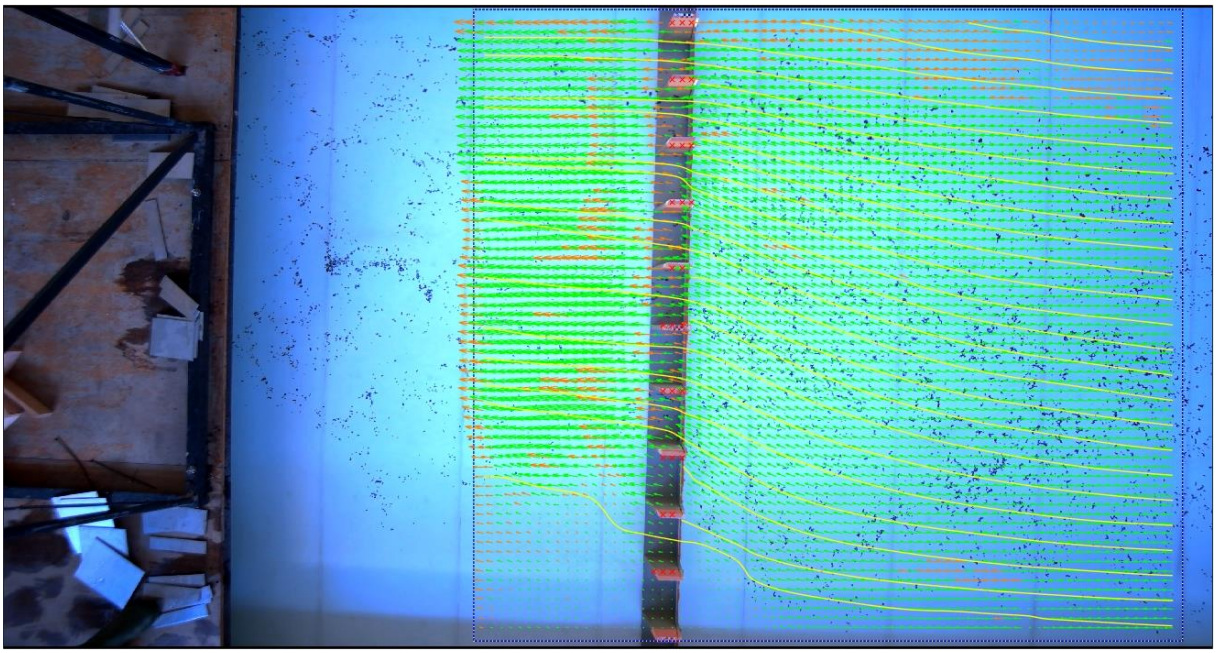

Figure 44 Velocity vectors including streamlines that were found using PIV on configuration 7.

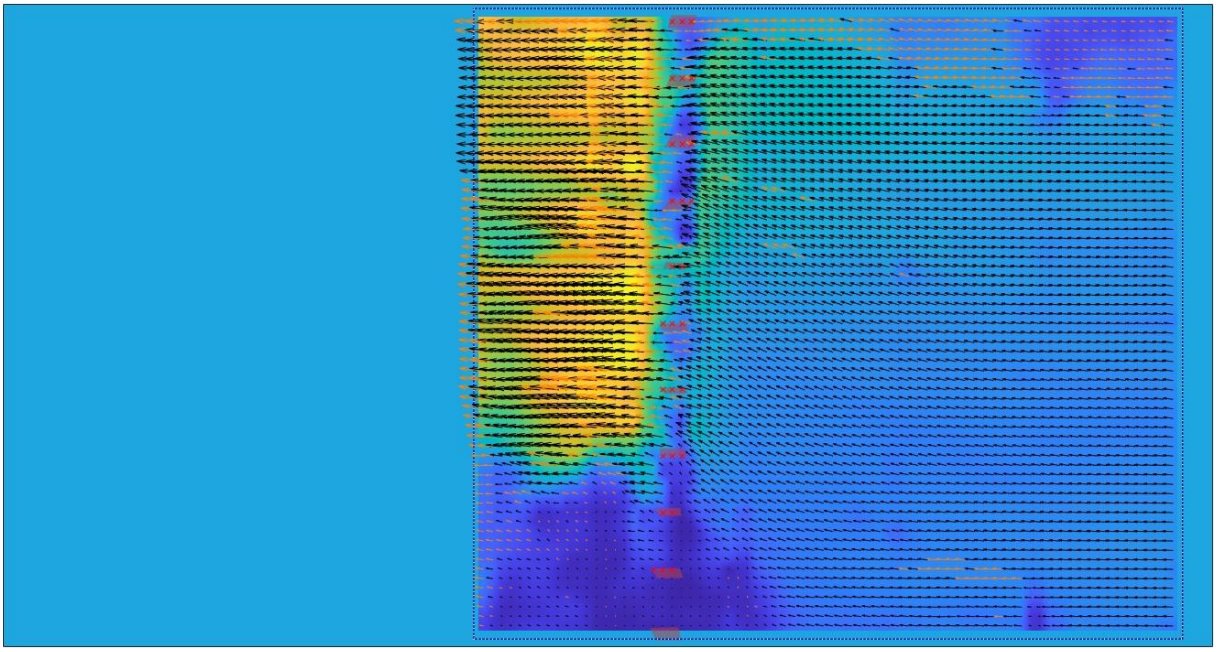

Figure 45 Qualitative velocity magnitude of configuration 7.

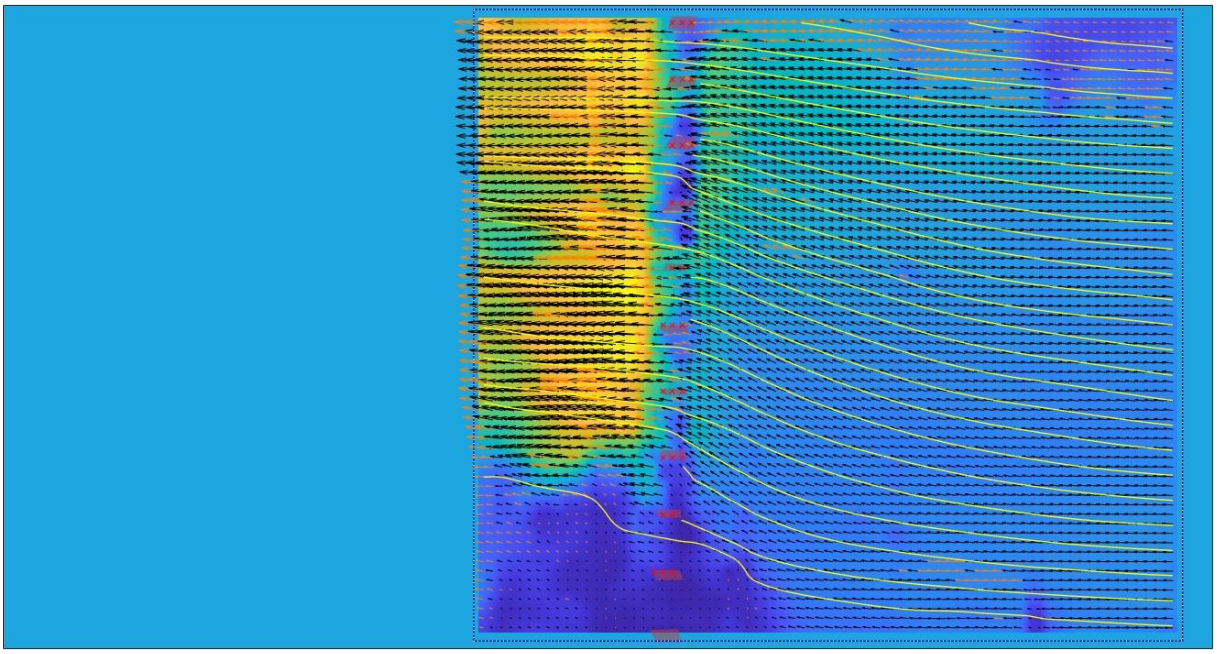

Figure 46 Qualitative velocity magnitude including streamlines of configuration 7.

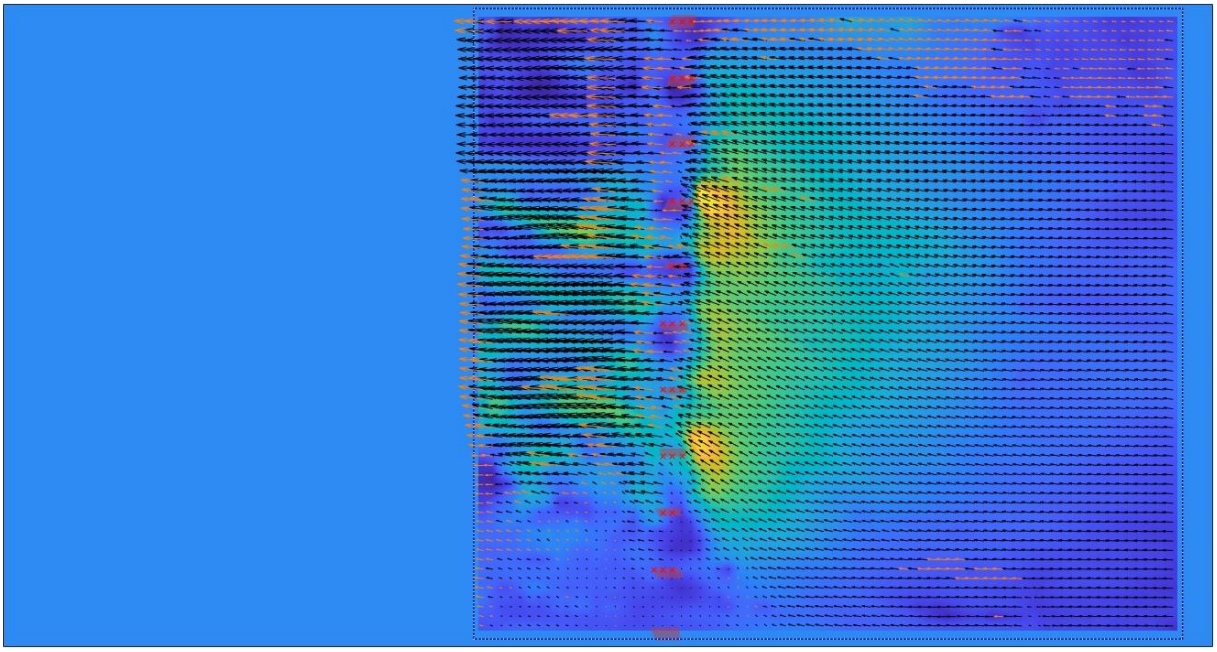

Figure 47 Qualitative magnitude of the lateral flow before and after the weir for configuration 7.

Appendix E: Analytical model

```python
class Weir:
    def __init__(self, height, *width):
        self.height = height + 0.003   # There is an extra 3 mm.

        standardwidth = 0.24
        self.width = width if width else standardwidth
    def __str__(self):
        return f"width: {self.width}, height {self.height}"
    def __repr__(self):
        return f"Weir({self.height}, {self.width})"
```

```python
class CompoundWeir:
    def __init__(self, weirs):
        self.weirs = weirs

        self.avg_height = sum(weir.height for weir in self.weirs) / len(weirs)

    def __len__(self):
        return len(self.weirs)

    def showWeir(self):
        x = 0
        weirNumber = 0
        for weir in self.weirs:
            plt.plot([x, x], [0, weir.height], "k-")
            plt.plot([x, weir.width + x], [weir.height, weir.height], "b-", label=f"Weir{weirNumber}")

            x += weir.width
            weirNumber += 1

            plt.plot([x, x], [0, weir.height], "k-")

        plt.ylim(top=.17)
        plt.xlabel("Width [m]", fontsize=15)
        plt.ylabel("Height [m]", fontsize=15)
        plt.xticks(fontsize=15)
        plt.yticks(fontsize=15)
#         plt.legend()

    def weirHeights(self):
        heights = np.zeros(len(self.weirs))
        i = 0
        for i in range(len(self.weirs)):
            heights[i] = self.weirs[i].height
        return heights
```

Individual approach "imperfect"

```
def calc_q_momentum_indv(q, Qtot, weirheights, h2):
    h2 = h2 * np.ones(len(weirheights))
    h2_ = h2 / np.cbrt(q**2/g)**3   # Non-dimensionalize by the q through each gate
    a_ = weirheights / np.cbrt(q**2/g)**3

    h1_ = np.zeros(len(a_))
    h0_ = np.zeros(len(a_))


    for i in range(len(a_)):
        a = 1
        b = 2*a_[i]
        c = a_[i]**2 - h2_[i]**2 - 2/h2_[i]
        d = 2

        values = np.roots([a, b, c, d])
        h1_[i] = values[1]

    h1 = h1_ * np.cbrt(q**2/g)**3
    h1_ = h1 / np.cbrt(q**2/g)
    a_ = weirheights / np.cbrt(q**2/g)

    for i in range(len(a_)):
        a = 1
        b = -(h1_[i] + a_[i] + 1/(h1_[i]**2))
        c = 0
        d = 1

        values = np.roots([a, b, c, d])
        h0_[i] = values[0]

    h0 = h0_ * np.cbrt(q**2/g)
    SOE = np.zeros(len(weirheights))

    for i in range(len(SOE)-1):
        SOE[i] = h0[i] - h0[i+1]
    SOE[-1] = np.sum(q * 0.24) - Qtot

    global h0_momentum_indv
    h0_momentum_indv = h0

#     print(h0)
    return SOE
```

```
def calc_q_carnot_indv(q, Qtot, weirheights, h2):
    h2 = h2 * np.ones(len(weirheights))
    h2_ = h2 / np.cbrt(q**2/g)
    a_ = weirheights / np.cbrt(q**2/g)

    h1_ = np.zeros(len(a_))
    h0_ = np.zeros(len(a_))

    for i in range(len(a_)):
        a = 1
        b = a_[i] - h2_[i] - 2/(h2_[i]**2)
        c = 1/h2_[i]

        values = np.roots([a, b, c])
        h1_[i] = values[0]

    for i in range(len(a_)):
        a = 1
        b = -(h1_[i] + a_[i] + 1/(h1_[i]**2))
        c = 0
        d = 1

        values = np.roots([a, b, c, d])
        h0_[i] = values[0]

    h0 = h0_ * np.cbrt(q**2/g)
    SOE = np.zeros(len(weirheights))

    for i in range(len(SOE)-1):
        SOE[i] = h0[i] - h0[i+1]
    SOE[-1] = np.sum(q * 0.24) - Qtot

    global h0_carnot_indv
    h0_carnot_indv = h0

#     print(h0)
    return SOE
```

Average approach "imperfect"

```
def calc_h0_momentum_avg(Q, weirheights, h2):
    qtot = Q / (12*0.24)
    a = np.mean(weirheights)

    h2_ = h2 / np.cbrt(qtot**2/g)**3
    a_ = a / np.cbrt(qtot**2/g)**3

    a = 1
    b = 2*a_
    c = a_**2 - h2_**2 - 2/h2_
    d = 2
    h1_ = np.roots([a, b, c, d])[1]

    h1 = h1_ * np.cbrt(qtot**2/g)**3
    h1_ = h1 / np.cbrt(qtot**2/g)
    a = np.mean(weirheights)
    a_ = a / np.cbrt(qtot**2/g)

    a = 1
    b = -(h1_ + a_ + 1/(h1_**2))
    c = 0
    d = 1
    h0_ = np.roots([a, b, c, d])[0]

    h0 = h0_ * np.cbrt(qtot**2 / g)
    return h0
```

```
def calc_h0_carnot_avg(Q, weirheights, h2):
    qtot = Q / (12*0.24)
    a = np.mean(weirheights)
    h2_ = h2 / np.cbrt(qtot**2/g)
    a_ = a / np.cbrt(qtot**2/g)

    a = 1
    b = a_ - h2_ - 2/(h2_**2)
    c = 1/h2_
    h1_ = np.roots([a, b, c])[0]

    a = 1
    b = -(h1_ + a_ + 1/(h1_**2))
    c = 0
    d = 1
    h0_ = np.roots([a, b, c, d])[0]

    h0 = h0_ * np.cbrt(qtot**2 / g)
    return h0
```

Calculation of discharge coefficients imperfect

```
def calculate_Cd_imperfect(compoundweir, h2, Qtotal):
    q0 = np.ones(len(compoundweir)) * (Qtotal/len(compoundweir) / 0.24)
    a = compoundweir.weirHeights()
    a_avg = compoundweir.avg_height
    cd = {}
#     H2 = h2 + (qtotal/h2) / (2*g)

    q = fsolve(calc_q_momentum_indv, q0, args=(Qtotal, a, h2))
    cd["momentum_indv"] = (Qtotal / (12*0.24)) / ((h2 - a_avg) * np.sqrt(2 * g * (np.mean(h0_momentum_indv) - h2)))

    q = fsolve(calc_q_carnot_indv, q0, args=(Qtotal, a, h2))
    cd["carnot_indv"] = (Qtotal / (12*0.24)) / ((h2 - a_avg) * np.sqrt(2 * g * (np.mean(h0_carnot_indv) - h2)))

    h0_momentum_avg = calc_h0_momentum_avg(Qtotal, a, h2)
    cd["momentum_avg"] = (Qtotal / (12*0.24)) / ((h2 - a_avg) * np.sqrt(2 * g * (h0_momentum_avg - h2)))

    h0_carnot_avg = calc_h0_carnot_avg(Qtotal, a, h2)
    cd["carnot_avg"] = (Qtotal / (12*0.24)) / ((h2 - a_avg) * np.sqrt(2 * g * (h0_carnot_avg - h2)))

    return cd
```

Individual approach "perfect"

```
def calc_cd_Rehbock_indv(weirheights, h0):
    cd = 0.611
    he = h0 + 1.1 * 10**-3
    for height in weirheights:
        if height < h0:
            cd += 1/len(weirheights) * he * 0.075 * 1/height
    return cd
```

Average approach "perfect"

```
def calc_cd_Rehbock_avg(weirheights, h0):
    _heights = []
    for height in weirheights:
        if height < h0:
            _heights.append(height)
    avg_height = np.mean(_heights)
    he = h0 + 1.1 * 10**-3
    return 0.611 + 0.075 * he/avg_height
```

Calculation of discharge coefficients perfect

```
def calculate_Cd_perfect(compoundweir, h0):
    cd = {}
    heights = compoundweir.weirHeights()
    cd["rehbock_avg"] = calc_cd_Rehbock_avg(heights, h0)
    cd["rehbock_indv"] = calc_cd_Rehbock_indv(heights, h0)

    return cd
```

Experiment results

```
def h0U_to_h0(h0_U):
    # Calibration values were measured in the lab using blocks of known height
    h0_U_calib = np.array([7.91, 6.96, 6.01, 7.98, 6.54])
    h0_h_calib = np.array([9.45, 11.83, 14.18, 9.23, 12.83])

    a, b = np.polyfit(h0_U_calib, h0_h_calib, 1)
#     h0_exp = a * (h0_U + 0.015/np.sqrt(200)) + b    #Testing the effects of a small deviation
    h0_exp = a * h0_U + b
    return h0_exp * 0.01 # cm to meters

def h2U_to_h2(h2_U):
    # Calibration values were measured in the lab using blocks of known height
    h2_U_calib = np.array([8.09, 7.13, 6.19, 8.19, 6.76])
    h2_h_calib = np.array([9.45, 11.83, 14.18, 9.23, 12.83])

    a, b = np.polyfit(h2_U_calib, h2_h_calib, 1)
#     h2_exp = a * (h2_U  - 0.015/np.sqrt(200)) + b
    h2_exp = a * h2_U + b
    return h2_exp * 0.01 # cm to meters


def expvalues_imperfect(h2_U, h0_U, Q, compoundweir):
    h0_exp = h0U_to_h0(h0_U)
    h2_exp = h2U_to_h2(h2_U)

    print("*IMPERFECT FLOW*\n"
         f"Measured values:\n"
         f"Downstream h2  : {h2_exp}\n"
         f"Upstream   h0  : {h0_exp}")

    a = compoundweir.avg_height
    q = Q / (12 * 0.24)
    cd = q / ((h2_exp - a) * np.sqrt(2 * g * (h0_exp - h2_exp)))
    return cd


def expvalues_perfect(h2_U, h0_U, Q, compoundweir):
    h0_exp = h0U_to_h0(h0_U)
    h2_exp = h2U_to_h2(h2_U)

    print("*PERFECT FLOW*\n"
         "Measured values:\n"
         f"Downstream h2  : {h2_exp}\n"
         f"Upstream   h0  : {h0_exp}")

    q = Q / (12 * 0.24)

    U = Q / (h0_exp * 3)
    a = compoundweir.avg_height
    H0 = h0_exp - a + U**2 / (2*g)

    cd = q / ((2/3 * H0) * np.sqrt(2/3 * g * H0))
    return cd
```

The weirs

```
compoundweir1 = CompoundWeir([Weir(0.05), Weir(0.05), Weir(0.05), Weir(0.05), Weir(0.05), Weir(0.05),
                              Weir(0.05), Weir(0.05), Weir(0.05), Weir(0.05), Weir(0.05), Weir(0.05)])

compoundweir2 = CompoundWeir([Weir(0.05), Weir(0.05), Weir(0.05), Weir(0.05), Weir(0.05), Weir(0.05),
                              Weir(0.10), Weir(0.10), Weir(0.10), Weir(0.10), Weir(0.10), Weir(0.10)])

compoundweir3 = CompoundWeir([Weir(0.05), Weir(0.10), Weir(0.05), Weir(0.10), Weir(0.05), Weir(0.10),
                              Weir(0.05), Weir(0.10), Weir(0.05), Weir(0.10), Weir(0.05), Weir(0.10)])

compoundweir4 = CompoundWeir([Weir(0.05), Weir(0.05), Weir(0.10), Weir(0.10), Weir(0.05), Weir(0.05),
                              Weir(0.10), Weir(0.10), Weir(0.05), Weir(0.05), Weir(0.10), Weir(0.10)])

compoundweir5 = CompoundWeir([Weir(0.05), Weir(0.05), Weir(0.15), Weir(0.15), Weir(0.05), Weir(0.05),
                              Weir(0.15), Weir(0.15), Weir(0.05), Weir(0.05), Weir(0.15), Weir(0.15)])

compoundweir6 = CompoundWeir([Weir(0.05), Weir(0.05), Weir(0.05), Weir(0.05), Weir(0.05), Weir(0.05),
                              Weir(0.15), Weir(0.15), Weir(0.15), Weir(0.15), Weir(0.15), Weir(0.15)])

compoundweir7 = CompoundWeir([Weir(0.05), Weir(0.05), Weir(0.05), Weir(0.05), Weir(0.10), Weir(0.10),
                              Weir(0.10), Weir(0.10), Weir(0.15), Weir(0.15), Weir(0.15), Weir(0.15)])

compoundweir8 = CompoundWeir([Weir(0.15), Weir(0.15), Weir(0.10), Weir(0.10), Weir(0.05), Weir(0.05),
                              Weir(0.05), Weir(0.05), Weir(0.10), Weir(0.10), Weir(0.15), Weir(0.15)])

compoundweir9 = CompoundWeir([Weir(0.10), Weir(0.10), Weir(0.10), Weir(0.10), Weir(0.10), Weir(0.10),
                              Weir(0.10), Weir(0.10), Weir(0.10), Weir(0.10), Weir(0.10), Weir(0.10)])

compoundweir10 = CompoundWeir([Weir(0.15), Weir(0.15), Weir(0.15), Weir(0.15), Weir(0.15), Weir(0.15),
                               Weir(0.15), Weir(0.15), Weir(0.15), Weir(0.15), Weir(0.15), Weir(0.15)])

compoundweir11 = CompoundWeir([Weir(0.05), Weir(0.05), Weir(0.05), Weir(0.05), Weir(0.15), Weir(0.15),
                               Weir(0.15), Weir(0.15), Weir(0.15), Weir(0.15), Weir(0.15), Weir(0.15)])
```

Appendix F: Planning

Week	Phase	Tasks	Deadlines
Week 1 **30 Aug – 5 Sept**	Orientation	- 1 Sep: initial meeting (online) - 2 Sep: meeting to finalize subject choice - Kick-off meeting - First supervisor meeting - Research proposal - Information literacy 2 - Reading previous BEPs and research	
Week 2 **6 Sept – 12 Sept**	Analysis	- 8 Sep: meeting starting note (online) - Literature research - Start sub-question I	6 Sept: Information literacy 2 6 Sept: Research proposal
Week 3 **13 Sept – 19 Sept**	Analysis	- 14 Sep: Lab introduction - 14 Sep: meeting - 16 Sep: meeting (online) - Prepare for experiments - Finalize sub-question I - Start sub-question II	
Week 4 **20 Sept – 26 Sept**	Experiments	- 21 Sept: meeting in the lab - 22 Sept: meeting D. Wüthrich - 23 Sept: time for questions - Collect data in water lab for the whole week - Process data - Continue sub-question II - Peer review - Finalize midterm report - Prepare midterm presentation	24 Sept: Midterm check
Week 5 **27 Sept – 3 Oct**	Elaboration	- 29 Sep: brief meeting - Finalize sub-question II - Start sub-question III - Discus results	27 Sept: Peer review 29 Sept: Midterm presentation
Week 6 **4 Oct – 10 Oct**	Elaboration	- 7 Oct: meeting - Finalize sub-question III - Discuss results	
Week 7 **11 Oct – 17 Oct**	Finalization	- 14 Oct: meeting D. Wüthrich (feedback) - Room for margins - Compile final report - Write discussion, recommendations, conclusion, preface, abstract - Make final adjustments and process feedback - Write ethics component	17 Oct: Ethics component
Week 8 **18 Oct – 24 Oct**	Finalization	- Prepare presentation	18 Oct: Draft final report 20 Oct: Presentation

Week 9 **25 Oct – 31 Oct**	Finalization	- Prepare ethics pitch - Add final corrections to report if necessary (?)	(?) Ethics component pitch
Week 10 **1 Nov – 7 Nov**		-	(?) Ethics component pitch Potential corrections